A Project Report

On

DESIGN AND FABRICATION OF ROBOTIC MANIPULATOR ARM USING COMPUTER VISION AND 3D PRINTING TECHNIQUES

Submitted to
Amity University, Uttar Pradesh

In partial fulfillment of the requirements for the award of the degree of Bachelor of Technology in Mechanical Engineering

By

ABHINAV SHARMA (A2399816016)
RISHABH BAVITHRAN SC (A2399816013)

Under the guidance of
Mr. Pritish Shubham
Asst. Professor

Amity School of Engineering and Technology
Amity University Uttar Pradesh
Noida (U.P.)

April-May 2020

DECLARATION

We, ABHINAV SHARMA and RISHABH BAVITHRAN SC, students of B.Tech (Mechanical Engineering), hereby declare that the project report titled "**DESIGN AND FABRICATION OF ROBOTIC MANIPULATOR ARM USING COMPUTER VISION AND 3D PRINTING TECHNIQUES**" which is submitted by us to the Department of Mechanical Engineering, Amity School of Engineering and Technology, Amity University, Uttar Pradesh, Noida, in partial fulfillment of requirement for the award of the degree of Bachelor of Technology in Mechanical Engineering, has not been previously formed the basis for the award of any degree, diploma or other similar title or recognition.

Noida

Abhinav Sharma

Rishabh Bavithran SC

Date: 19/05/2020

Name and Signature of Student(s)

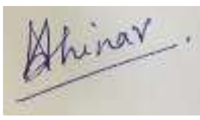

CERTIFICATE

On the basis of declaration submitted by ABHINAV SHARMA and RISHABH BAVITHRAN SC, student(s) of B. Tech (Mechanical Engineering*)*, I hereby certify that the project titled "**DESIGN AND FABRICATION OF ROBOTIC MANIPULATOR ARM USING COMPUTER VISION AND 3D PRINTING TECHNIQUES**" which is submitted to Amity School of Engineering and Technology, Amity University, Uttar Pradesh, in partial fulfillment of the requirement for the award of the degree of Bachelor of Technology (Mechanical Engineering), is an original contribution with existing knowledge and faithful record of work carried out by him/them under my guidance and supervision

.

To the best of my knowledge this work has not been submitted in part or full for any Degree or Diploma to this University or elsewhere.

Noida

Date

Signature of Guide
(**Mr. Pritish Shubham**)
(Asst. Professor)
Amity School of Engineering and Technology
Amity University, Uttar Pradesh

DECLARATION FORM

We, ABHINAV SHARMA (A2399816016) and RISHABH BAVITHRAN SC (A2399816013), students of B.Tech (Mechanical Engineering), batch 2016-2020, Department of Mechanical Engineering, Amity School of engineering and Technology, Amity University, Noida, Uttar Pradesh, hereby declare that we have gone through project guidelines including policy on health and safety, policy on plagiarism etc.

Date: 19/05/2020

Place: NOIDA, U.P **Student Signature**

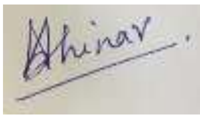

ACKNOWLEDGEMENT

We, Abhinav Sharma and Rishabh Bavithran SC, students of Amity University, Noida, would like to express our gratitude to Mr. Pritish Shubham sir, our project guide, for supporting the project throughout and to guide me at every step during the course of our project.

We would like to thank our Head of Department Prof. (Dr.) Basant Singh Sikarwar for providing us with every facility and equipments required for the experimental work and successful completion of our project.

Lastly, we would also thank other people involved who have helped us in every way for successful completion of our project.

This experience was very useful in our personal growth. It helped us in understanding the essentials of working in professional environment and finding useful outcomes to the problems faced.

CONSENT FORM

This is to certify that we, ABHINAV SHARMA and RISHABH BAVITHRAN SC, students of B.Tech (Mechanical Engineering) of 2016-2020 batch presently in the VIII Semester at Amity School of Engineering and Technology, Domain of Engineering and Technology, Amity University Uttar Pradesh, give my consent to include all my personal details (i.e. Name, Enrollment ID, etc.) for all accreditation purposes.

Place: Noida

Signature of the Student Date:

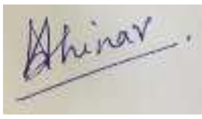

Enrollment Number A2399816016

A2399816013

LIST OF FIGURES

LIST OF TABLES

LIST OF EQUATIONS

1 Contents

1 INTRODUCTION

We took up this project because AI and robots are going to play a major role in the coming years. Robots that can work rigorously with very little or low errors are trending and will see a major boom in the years to come. Our goal is to be part of and contribute to the industrial revolution 4.0 with our robot. The robot we are interested in is a pick and place with vision sensor.

Based on information from the already developed industrial robots with their pros and cons, a basic idea of the design of the robot was drafted.

The existing industrial robots are not completely automated. The robot which we are trying to achieve is fully automated with the help of computer vision and image processing.

The robot we plan on developing will be 3D printed and will use computer vision to learn and understand the surroundings to perform tasks. Both 3D printing and computer vision play a major role in the 4.0 revolution. The robot will be able to perform pick and place tasks through information input from cameras.

1.1 Beginning with the Project work

After establishing our end goal, the requirements of the project were laid out with a detailed layout of the questionnaire about the robot itself. This stage ended with a detailed layout of the robot capabilities.

Building upon the robot capabilities, a detailed workflow and procedure planning was developed based on requirements and understanding of various topics. Gantt chart was formulated at this stage.

1.2 Robot Manipulator

The term manipulation refers to handle or control of the physical objects made to the world around us purely speaking in robot terms.

The industrial robot is based on the concept of hard robotics. Hard robotics deals with the use of hard and rigid bodies whose degree of freedom is an exact measurable value. Soft robotics uses materials that can change shape and are not rigidly defined and as a result their degree of freedom cannot be determined. A robot manipulator makes use of rigid links which are arranged together using joints.

An industrial robot arm manipulator comprises of a number of rigid links and joints arranged in a certain fashion allowing them to move to interact with the surroundings. The interaction will mainly depend on the constraints placed by the degree of freedom of the structure, link length and material, power of actuation. A robot manipulator arm is capable of pushing, grasping, moving, throwing, dropping and many more actions whatever the design allows and was designed for.

1.2.1 Types of Robotic Manipulator

There are many types of robot manipulators. To name a few popular ones:[3]

A. Articulated Robot : This robot has rotary joints with twisting joint in the base. These are the most popular kind of industrial robots because of the degree of freedom it provides and the workspace envelope. Each joint is called an axis. These kind of robots usually have 6 axes but there are robots with up to 10 as of now.

Figure 1 Articulated Robot

B. Cartesian Robot : The joints in this robot provide linear motion. It follows the X,Y,Z Cartesian coordinate system. Some robots may have a wrist attached in the end for flexibility. Sometimes they are called as gantry robots. The primary difference between a gantry robot and a Cartesian robot is that the gantry robot has 2 bases. Rest all the joints are linear as found in Cartesian robots.

Figure 2 Cartesian Robot

C. Cylindrical Robot: These robots have a cylindrical workspace. The motion is provided by twisting and prismatic joints. Twisting joint at the base and at least one prismatic joint to connect the links provides a unique combination and thus a cylindrical workspace is obtained. It is rarely used in current times

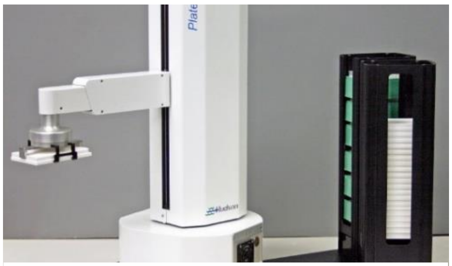

Figure 3 Cylindrical Robot

D. Polar Robot: These robots have a very specific combination of twisting joint at the base followed by two rotary joints for connecting the links and a prismatic joint at the end. This combination manages to form axes relating to the polar coordinate system and thus the name. It has a spherical workspace.

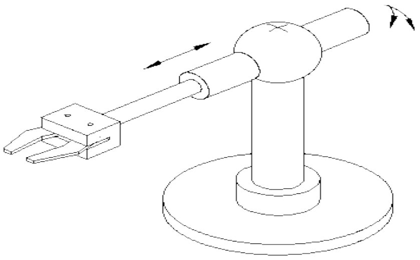

Figure 4 Polar robot

E. SCARA robot: This robot is predominantly cylindrical in design. These robots are designed to provide compliance on a single plane. It has 2 parallel joints which helps accomplish the aforementioned.

Figure 5 Scara Robot

F. Delta robots: These robots have a spider like leg arrangement mainly used for categorizing or pick and place task. These legs are connected to a parallel base like arrangement. This kind of arrangement helps it achieve a dome shaped workspace.

Figure 6 Delta Robot

1.2.2 Pros and Cons of Robotic Manipulator

Pros

1. Fasten process
2. Working in harsh and hazardous environments without need of comfort
3. Elimination of human errors
4. Performing dangerous tasks
5. Repeatability of process
6. No need of break and no distractions
7. No compromise in quality with long run
8. Less operating cost
9. No need for supervision and monitoring of tasks
10. Can reach areas with difficult accessibility with ease and without delay

Cons

1. Needs regular maintenance
2. Need of experienced programmer
3. Manipulators with AI are intelligent but not as intelligent as humans
4. Wear with time
5. High initial cost of setup
6. Large area needed for setup

1.2.3 Area Of Use Of Robotic Manipulators

Use of manipulators is not restricted to one field. Nowadays every domain of the research, service and industrial sectors are upgrading to robotic and automation. Robotic manipulators are majorly used for automation of industries. These robotic manipulators are also used where:

1. it is inaccessible or time consuming for the human to reach,
2. the process needs to be fastened,
3. the human error cannot be tolerated,
4. human safety is an issue the working environment is not favorable for human kind,
5. it is need of continuous quality assurance with repetitive activity.

1.3 Applications of robotic manipulators

Manipulators can be used in various applications such as medical, industrial, military, space activities etc. With the upgrading robotic sectors, the research and invention of the robots with artificial intelligence is not far. This advancement in the robotic sector will enhance and vastly extend the limits of use of the robots in various sectors.

With the introduction of this technology of Artificial intelligence in the robotic sector will ease mass sectors of the society. They can be used to clean the sewers, handle hazardous chemicals and other various automated household, official and industrial activities.

Robotic manipulators at present are used in various sectors of the society mentioned below:

1. **Industrial sectors:** in industrial sectors there is a possibility of 100% automation. As of now industries are shifting toward the automation steadily in this era of Industrial Revolution 4.0 because of the numerous advantages it has over traditional methods. Robotic technology is used by the industry for rapid manufacturing processes where the process to be performed is repetitive and fast. Industries use the robotic manipulator for inspection and error rectification, welding, material handling, assembly, pick and place and some machining operations.

Figure 7 Industrial Robots

2. **Medical Sector:** The need for robots in medical sector arises from the enhanced capabilities of robots in performing surgeries, diagnosing, rehabilitation and sanitation procedures. There are mainly 6 areas where medical robots are used.
    a. **Telepresence:** The robots are used for diagnosing patients. A patient can only be treated if the problem has been found. So the diagnosing must be accurate. With the increasing AI technologies, a robot will be able to pin point the exact cause of the problem in patient which can save the life of a critical patient where time is crucial.

Figure 8 Telepresence used by physicians

    b. **Surgical Assistance:** Surgery requires high level of precision and accuracy. Any miscellaneous movement cannot be tolerated. Humans are prone to such errors and cannot be avoided. Minor hand shaking, accuracy based on the human eye are all errors that can risk the life of the patient in some critical procedures. The robots overcome and eliminates all such possibilities.

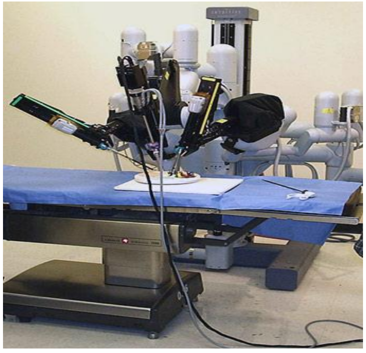
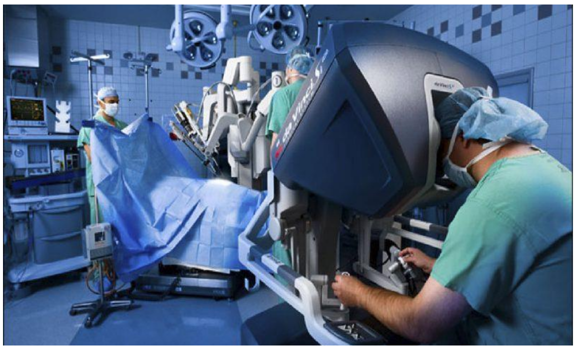

Figure 9 Surgical Assisted Robots

c. **Rehabilitation robots:** People with disabilities require assistance. This assistance is provided by robots which provide mobility and strength. The ease of re-programmability in robots can adapt to specific patient disabilities thus helping them to improve the quality of life.


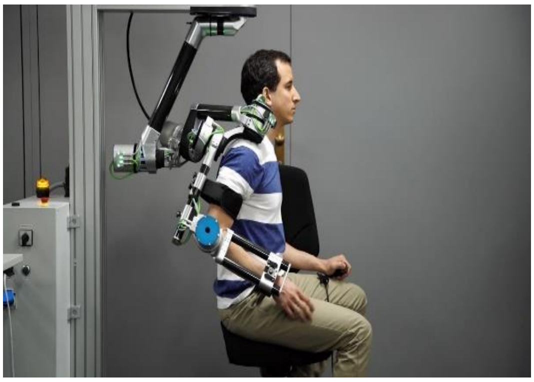

Figure 10 Rehabilitation Robots

d. **Medical transportation robots:** These are simple tasks like medicine, report collection and handling. This helps in optimizing the communication between doctors, nurses and patients and in general co-ordination of the hospital.


Figure 11 Medical Transportation Robots

e. **Sanitation and disinfection robots:** Some diseases are contagious. Robots can be used in such cases. For the purpose of disinfection or sanitation where physical touch with the patient is required, using robots in such cases is safe for both the patient and the doctors/nurses assisting the procedure and prevents any further spreading of those diseases.

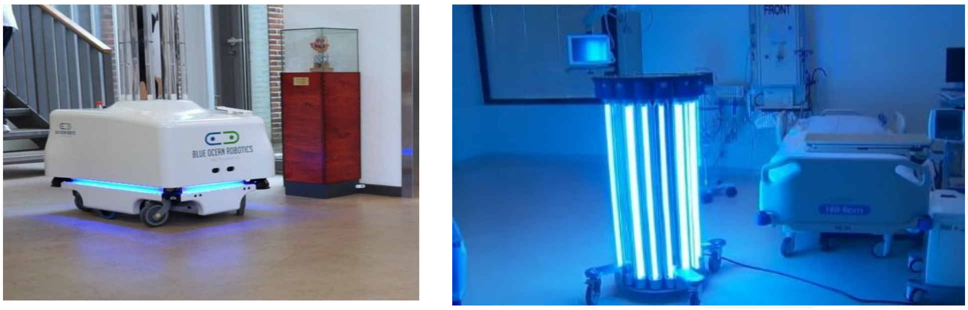

Figure 12 Sanitation and Disinfection Robots

f. **Robot prescription dispensing systems:** These robots reduce the manpower required for assisting a large group of patients because of their high speed and accuracy. Tasks like vaccinations, injections and many more are carried out by robots.

Figure 13 Prescription and dispensing Robots

3. **Space sector:** The atmosphere of the earth is the only known place where humans can survive. Space has extreme conditions. Robots are used extensively in such cases. Space exploration, collection of data for research and expecting to extend life beyond earth. Before going to a new space position to make sure of the safety of humans these robots are sent to check climate and temperature conditions of that position.

Figure 14 Space Research Robots

4. **Military sector:** The use of robots as a medical supply transportation, mission ground assistance, connectivity of soldiers with the headquarters, diffusing bombs, fighting against terror activities, surveillance purposes and dealing situations in nuclear bomb affected areas has helped the arm forces of the nation to a great extent.

Figure 15 Military and Anti-terror Robots

5. **Agriculture sector:** The agricultural sector has significantly benefitted by the evolution of robotic technology from a few years. Nowadays robots have fastened the agricultural activities by the use of automation and decreasing human intervention in the agricultural activities. Processes such as harvesting and picking, weed control, autonomous mowing, pruning, seeding, spraying, thinning, sorting, packing and phenotyping. In agricultural sector the robots are also used to collect samples from different tough regions to check for various factors and ingredients of the soil collected.

Figure 16 Agricultural Robots

6. **Household sector:** In household sectors with the introduction of technology of smart homes where the automation is done using robots. The robots are used for cleaning of swimming pools and floor of the house, picking up litters and lawn mowing activities. In the upcoming technology by the research in robotics the household activities will be made automated to a large extent.

Figure 17 Household Robots

2 LITERATURE REVIEW

Since the dawn of humanity our kind has been evolving. We understood that we needed food to survive and hence before any industrial revolution our societies were mainly focused on agriculture.

The first industrial revolution brought about the age of mechanical production. This age derived its power from steam. In 1760, societies started transforming from agrarian to urban. Factories started growing thus bringing about the community change. Many people worked in factories and thus paving way for the life we know today.

The second industrial revolution took place in the early 20th century. It was an age of science and mass production. A number of key inventions that paced the manufacture of products were developed. The transport industry also saw a major boom in this stage with the development of gasoline engine and airplanes. The key invention for speeding up the manufacture was the assembly line. It was because of these developments that people started looking for jobs and thus started moving to urban areas leaving behind their rural home towns. The urbanization we know of today was brought by the second industrial revolution.

The third industrial revolution was the age of digitalization. Things that used analog waves were starting to digitize. Automation started in this era with electronics and information technology making supply chains global.

The 4th industrial revolution is underway which takes automation to a whole other level. It is about the development of machines that are able to think for themselves to perform tasks without any human interaction which is termed as Artificial Intelligence. Apart from this, gene editing, nanotechnology is also a part of this revolution but the focus of our project is towards the automation of manufacturing sector.

In the era of 4th industrial revolution where the evolution of the industries are more focused on automation. This automation is required for meeting the increasing demands of the products in each sector. Land resource being among the one of the limited resources, the allocation of this resource is to be efficiently divided for a better life. The land allocated should be utilized to its full potential for the purpose. This is only possible if the each sector is technologically updated. By automation the industries production rate will increase due to reducing the non-production time to a large extent.

Robotics is a vast field with a wide variety of applications. In this project we will be focusing on the industrial robots that help in the manufacturing sector. The various types of robots on the basis of configuration of the joints are:

1) Articulated manipulator: This robot has all joints as revolute. This is extremely capable in terms of positioning and approachability.
2) Cartesian Robot: All the joints are prismatic in the x, y and z directions and thus not allowing much freedom in the angle of approach.
3) Cylindrical Robot: This robot has a revolute and prismatic joints and thus giving it a cylindrical workspace.

4) Polar Robot: This robot has a twisting joint at the base followed by two rotary joints and then a prismatic joint at the end giving it a spherical workspace.
5) SCARA Robot: This is designed for working on a single plane through a series of revolute joints.
6) Delta Robots: It has a spider like shaped legs acting as links allowing for a dome shaped workspace with maximum angle of approach.

This literature review will consist of findings for robots and programming languages that can be used or already being used in the manufacturing sector.

In a book by J.M Skowronski, he has stated that the robot must be able to reach between two points in a smooth path while avoiding any stationary or moving obstacles. They are also expected to have a good accuracy and perform the tasks within the provided space and provided time frame. This task is full of unknown variables throughout the functioning of the robot. These robots must be robust and is absolutely necessary that they have a constant closed loop feedback system to adapt to every error possible. This book covers various insights on how to achieve all the above stated.

The main purpose of this literature review is to study and understand the existing similar industrial applications robotic manipulators, understanding computer vision better and integration of both the techniques to build a smart self-functioning industrial robot. The ideas and techniques that will be suitable for our specific use case can be extracted from the existing studies made.

Vision-based Robot Manipulator for Industrial Applications

A Scorbot ER-4 Plus is controlled by an Advance Control Language. It is a robot that has the option to be preprogramed or controlled manually for any use case. This paper focuses mainly on integrating the functions of MATLAB and the ACL of the Scorbot ER-4 Plus to perform pick and place tasks based on the shape, size and colour of the object.

A detailed plan is laid out to capture the image and extract as much information as possible from a single image. The Red Green Blue format is used in MATLAB and as such these three colour channels are manipulated to perform thresholding operations, finding the centroid of the object and many more. The computer vision program is programmed as such to detect the shape, colour and area of the object. Once the objects are identified and separated, the computer can now understand the differences and these differences can be further fed into the ACL to perform pick and place tasks. This method uses a camera mounted on the robot itself so its field of vision is quite narrow. It cannot look beyond its current position and angle. The distance and depth mapping is also not used which may be required for further intricate applications in industrial applications. **[1]**

Neural Network Model for Identifying Workspace, Forward and Inverse Kinematics of the 7-DOF YuMi 14000 ABB Collaborative Robot

Morteza Alebooyeh & R. Jill Urbanic studied the YuMi 14000 ABB collaborative robot which has a degree of freedom of seven. The author mentioned the reason for such a high degree of freedom to be the addition of multiple angles of approach at one point in the dexterous workspace giving it advancement in flexibility of the robot. This kind of approach is very useful in order to globalize the use of the robot in every sector. He also explained the use of neural network being better than programmed robots to make a learning robot and therefore building up artificial intelligence. We will try to in-corporate neural network other than using programming to make the robot perform monotonous task. Mitsubishi RV-M1 robot uses Denavit-Hartenberg table to determine the position of the end effector with respect to the base which is convenient and an effective way to approach with the positioning of the end effector. The publisher also shows the dexterous workspace of the robot to list out the applications of the robot and its feasibility. The same approach can be used to show the dexterous workspace of our design which will help us to restrict the movement of link to completely avoid overlapping of the links if present and also any unnecessary collision with the ground. **[2]**

The conference papers and publishers cover various methods to control a robot and build an interface between the robot's joint variables and the visual feedback. The method to determine the joint variables with respect to the Cartesian co-ordinates which was used in the above papers can be implemented in this project. The requirement of microcontrollers and programming languages that can be used for computer vision, kinematics and stepper motor control has to be looked into further for use in this project.

3 DESIGN METHODOLOGY

3.1 Overview

Movement of the robot will be achieved using stepper motors and drivers. The robot will be a desktop size robot capable of picking and placing objects within 1Kg inside a radius of 60-70 cm from the center of radius of the base of the robot with 4 degrees of freedom. Links of the robot will be 3D printed. Average link length was calculated for the robot to achieve a reach of 60-70 cm on the table level. All the joints in the robot will be revolute.

3.2 Degree of Freedom of a rigid body

Configuration of a robot: It is the positions of all the points in a robot. Configuration of a robot is widely used to determine the capabilities of a robot. The robot we plan to construct is made of rigid bodies. These rigid bodies are called links. These links are joined together by joints. Since the body and structure is rigid, only a few numbers are required to define the configuration of a robot unlike objects that are soft and in robot terms that comes under **soft robotics**.

The configuration space: It is the space of all the configurations of a robot.

Degrees of freedom: The dimension of the configuration space. It is minimum number of real numbers required to represent the configuration.

Since a robot consists of rigid bodies, the number of degrees of freedom of the robot is determined by the number of degrees of freedom of a rigid body.

To determine the number of degrees of freedom of a rigid body in free space, consider a cuboid and 4 points as shown in figure.

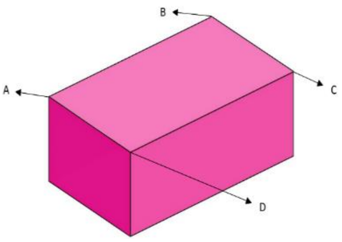

Figure 18 Movement of rigid body with constraints

The representation of point **A** requires three numbers in a 3 dimensional space which are the x,y and z co-ordinate.

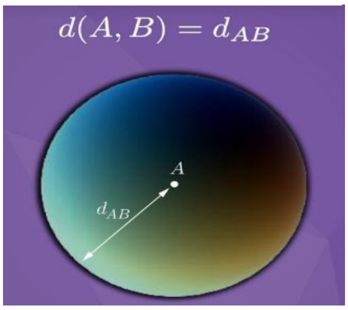

Figure 19 Degree of freedom 1

Upon fixing point A, the representation of point **B** requires only 2 numbers. As the body is rigid the distance between **A** and **B** is always constant and hence the point **B** always lies on the surface of a sphere with its centre lying at **A**. To represent a point on the sphere only latitude and longitude values are required. The constraint on point **B** is the point **A**.

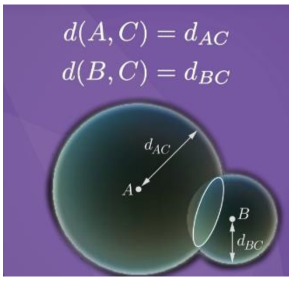

Figure 20 Degree of freedom 2

For determining the co-ordinate space for **C** two spheres are required. It is the space obtained by fixing point **A** and point **B.** It is obtained by drawing the configuration space of **A, C** which is by obtained by fixing point **A** and **B, C** which is obtained by fixing point **B**. They are similar to the way sphere formed by **A** and **B** previously. Now the intersection circle for these two spheres will give the configuration space for **C.** A circle can be represented by 1 degree of freedom.

After fixing the points **A**, **B** and **C** we can come to the conclusion that point **D** cannot move.

Point A has no constraints and thus can be chosen freely. Point B has a single constraint which is the point **A**. Point **C** has 2 constraints and **D** is thus completely constrained as **A**,**B** and **C** are fixed and has no degree of freedom. This has been summarized in the *table 2* given below

Table 1 Points and their kinematic properties

Point	Co-ordinates	Independent constraints	Real Freedom
A	3	0	3
B	3	1	2
C	3	2	1
D	3	3	0
TOTAL			**6**

In a 3 dimensional space, a rigid body has 6 degrees of freedom. 3 of them can be represented by **x**, **y** and **z** co-ordinates and the rest are angles which are called **roll, pitch** and **yaw**.

Therefore the degree of freedom for any system can be represented as

Degree of Freedom = ∑ (freedom of points) – number of independent constraints acting on the point

For a general mechanism we can write this as

Degree of Freedom = ∑ (freedom of bodies) – number of independent constraints acting on the point

Using this information we can formulate the degree of freedom of any general mechanism.

In a robot, the degrees of freedom are mostly determined by the type of joints that bring together the links. The degrees of freedom for the most common types of joints are as follows:

Revolute Joint:

Here the link 2 can move in direction with respect to the position of link 1. It has 5 constraints placed on it that is out of the 6 degrees of freedom available it can move in only 1 direction. It only requires 1 value which is the angle between the links to determine the position of link 2. *(Figure 20)*

Prismatic Joint:

The link 2 can move only in 1 direction with respect to 1. It can slide along link 1 as seen in *Figure 21***.**

Twisting Joint:
The Twisting Joint has 1 degree of freedom. The output axis is aligned with the input axis and rotates around it. As seen in *Figure 24*, the link moves around the axis of link 1.

Table 2 Types of Joints and their DOF

Joint Type	Degree of Freedom	Constrains between the two planar rigid bodies	Constraints between two spatial rigid bodies
Revolute Joint (R)	1	2	5
Prismatic Joint (P)	1	2	5
Helical Joint (H)	1	-	5
Twisting Joint (T)	1	-	5
Cylindrical Joint (C)	2	-	4
Universal Joint (U)	2	-	4
Spherical Joint (S)	3	-	3

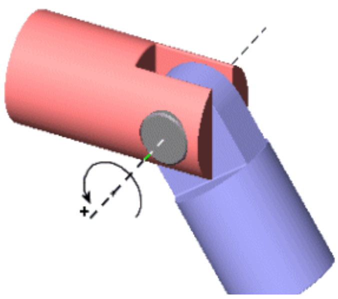
Figure 23 Revolute Joint

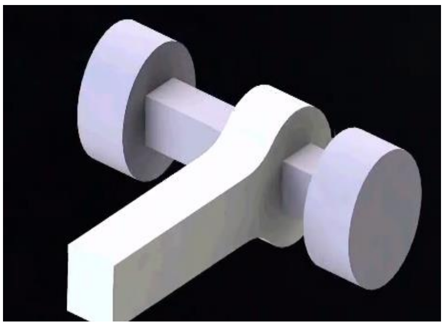
Figure 22 Prismatic Joint


Figure 21 Universal Joint Figure

Universal Joint:

The Universal Joint has 2 degrees of freedom relative to the first body. It has 4 constrained motions. *(Figure 22)*

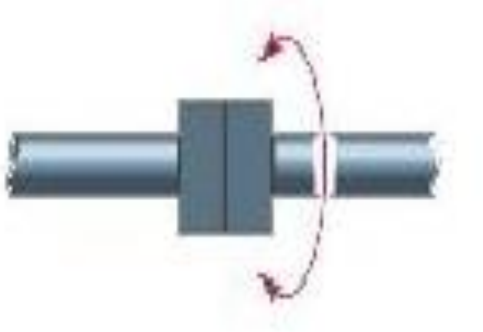

Figure 25 Twisting Joint

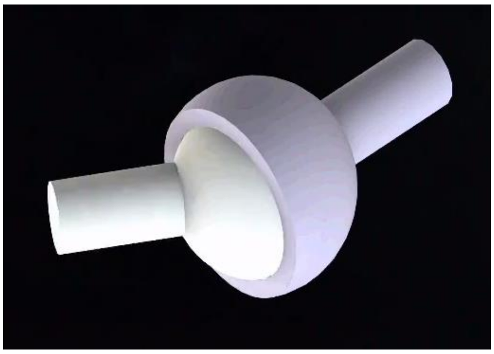

Figure 24 Spherical Joint

Spherical Joint:

The Spherical joint is similar to the universal joint except that the 3rd degree of motion is provided by the rotation around its own axis of link 2. *(Figure 23)*

Helical Joint:

The Helical Joint has a degree of freedom of 1. *(Figure 26)*

Cylindrical Joint:

The Cylindrical joint has a configuration such that link 2 can move along the axis like a prismatic joint and rotate about the axis of link 1 as well. *(Figure 25)*

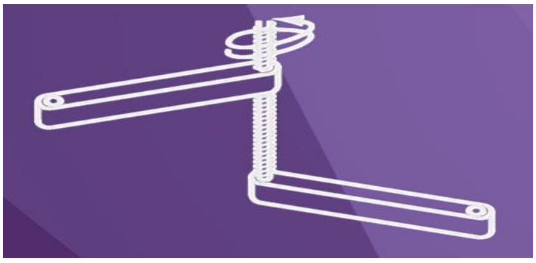

Figure 26 Helical Joint

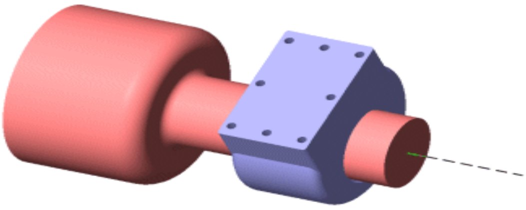

Figure 27 Cylindrical Joint

Using the equation **Degree of freedom = ∑ (freedom of bodies) – number of independent constraints** and the above table a general equation to find the degrees of freedom of a robot can be formed.

N = number of links, including ground

J = number of joints

m = degrees of freedom of a single body (m = 6 for spatial body, m = 3 for planar body) therefore the general equation can be written as

$$\boldsymbol{Degree\ of\ freedom = m(N-1) - \sum_{i=1}^{J} c_i}$$

Equation 1 General degree of freedom

Here (N – 1) gives the total number of links other than ground. Now m (N – 1) gives the total degree of freedom of the bodies without any constraints.
$\sum_{i=1}^{J} \boldsymbol{c_i}$ *provides the number of constraints given by "**J**" joints.*

As the number of constraints provided by each joint number "***i***" is the difference between degrees of freedom of a single body minus the degree of freedom allowed by that joint (m – degree of freedom of that joint), therefore $\boldsymbol{c_i}$ can be replaced by m - f_i where f_i is the degree of freedom of joint number "***i***".

Rewriting the *Equation 1* we get

$$\boldsymbol{Degree\ of\ freedom = m(N-1) - \sum_{i=1}^{J} (m - f_i)}$$

Equation 2 Modified degree of freedom

Rearranging the above equation we get

$$\boldsymbol{Degree\ of\ freedom = m(N-1-J) + \sum_{i=1}^{J} f_i}$$

Equation 3 Rearranged degree of freedom

The above equation is called **Grubler's formula**. This equation assumes that the constraints provided by the joints are independent.**[4]**

3.3 Designing of the robot

Using CAD software, a design was computed for 4 degrees of freedom with maximum possible workspace area. The design was simulated using Altair Inspire. The flaws of each design iterations lead to the development of the next design iteration overcoming the previous flaws. A tracing point is used to track the positions of the end effector at various times. Motor used is set at 60 RPM with fixed time limits for each motor. The general waveform for the motors used in motion analysis of the structures is given in **Fig 2.** The analysis is done for a 10 seconds for finding the torque requirement of the motors. The end effector position determinations are carried out with various possible combinations of angular accelerations for maximum possible end effector position combinations.

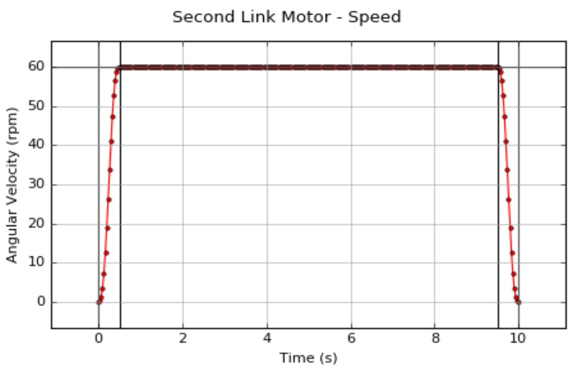

Figure 28 Motor Angular velocity vs Time General Waveform used

4 Analysis And Simulation

4.1 Kinematic Analysis of Robot Steps Involved

Using Altair Inspire, the solid model can be analyzed on various aspects. The results of the analysis can be further used to remove excess material, reduce strains using the information, and get an understanding of the required power for electrical components and many more. The kinematic analysis can be observed in real time for any of the variables either in the material or any electrical equipment. The specialty of this software is that it removes the material automatically according to the constraints given by the user which saves a lot of re-designing time and resources. This software has been used to analyze the robotic manipulator arm for troubleshooting and making the design as efficient as possible before fabrication.

Altair Inspire allows basic manipulation of geometry within the software itself. It also allows importing various CAD file extensions to be imported to the software for further analysis. The software recommends parasolid file type (.x_t) imports. The design can be modelled on any CAD software.

The procedure for complete analysis of the model was carried out as follows.

1) Run Altair Inspire

The menu on top has seven main categories - **File, Edit, View, Geometry, Structure, Motion and Manufacture.** Each category has a unique in various designing stages which we will use during the kinematic analysis procedure.

Figure 29 Seven main categories of top Menu Bar

2) On the above menu select **File** and then **Import** from the drop down menu.

3) In the dialogue box that opens, locate the CAD model, preferably parasolid (.xt) Once the design is imported, information on the various parts of the robot can be viewed from **Model Browser** from the left side on screen. Here the assembly tree is visible and all the changes made in the Inspire will also be seen in this window. The specifications, changes will be visible in the Model browser window.

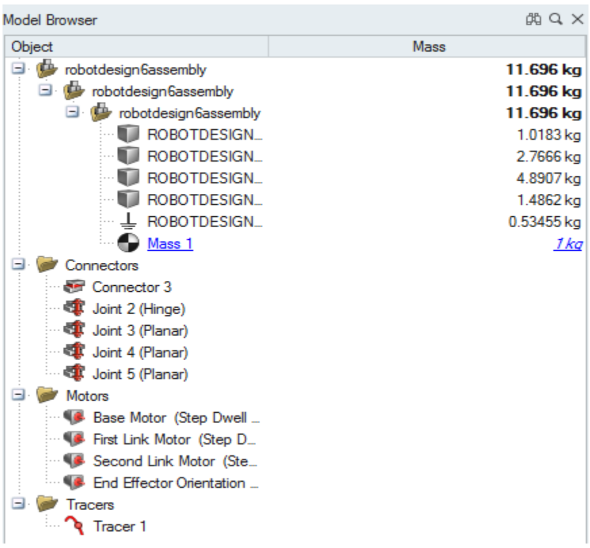

Figure 30 Model Browser

4) Right click on the assembly and click on **Material** from the drop down menu and select **Plastic (ABS).**

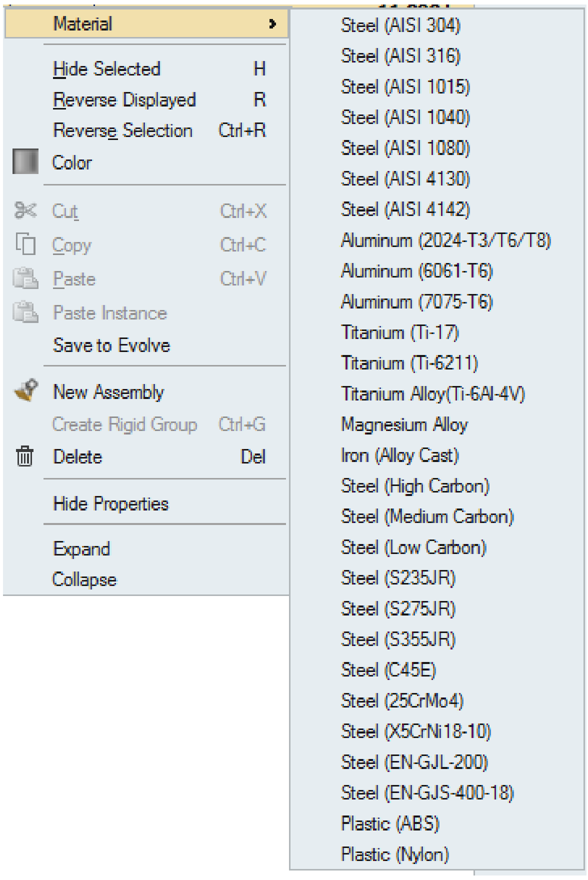

Figure 31 Material Selection

Plastic (ABS) is the material the 3D printer will use for fabrication of the model.

It is absolutely necessary to **Ground** certain parts to work on it.

5) Under the top menu **Motion**, a number of options open. Click on **Ground** and select the base (part 1) to ground it.

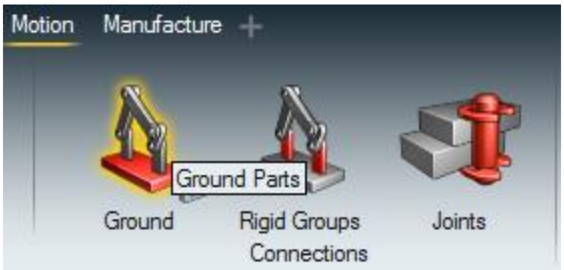

Figure 32 Motion Analysis tools

The next step is to define the contacts between various linkages. There are 3 types of contacts between various linkages. **No contact, contact** and **bonded.** No contact is used when the linkages have no contact between them. Contact is used when the linkages that touch each other have movement between them and bonded is chosen when the linkages are completely bonded with no relative motion between them.

6) Click on **Structure** from the menu and select **Contacts**. The software will automatically analyse the model and based on the requirements we can select if the touching pairs are **No contact, contact** or **bonded. 4** contact areas are highlighted with some specific colour. Each type of contact has a colour assigned to it as visible in the top left corner of the design area. Move the mouse pointer to the highlighted or coloured areas and select **Contact** for every highlighted area.

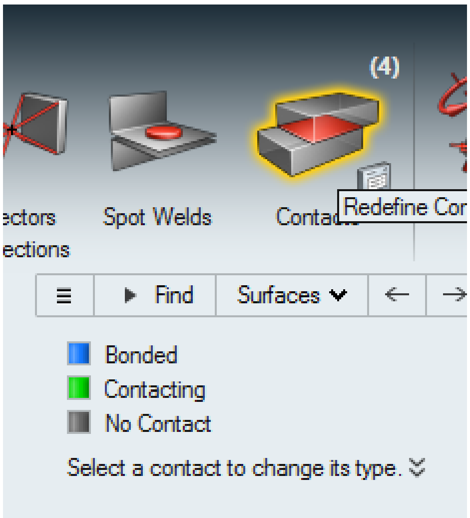

Figure 33 Constraint tools

The next step is to define the joints. The three types of joints are **Locked, Active and Free.** Locked joint doesn't allow motion between the joints. Active joints have to be further specified as to which type of joint for letting the software know the type of motion between them.

7) Click on **Motion** tab and select **Joints.** The colour highlights the detected possible joints. Move the mouse pointer over the joints and click on each of them to define the type of joint

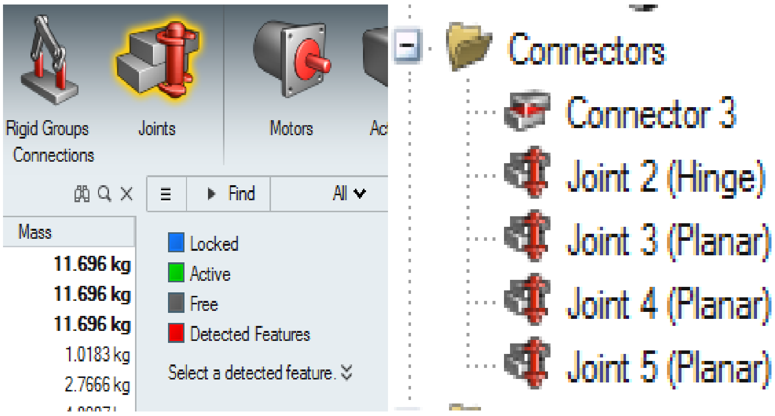

Figure 34 Various Joint Creation

The joint between **ROBOTDESIFGNPART1** and **ROBOTDESIGNPART2** is to be chosen as **Hinge.** The other three detected joints are to be defined as planar joints.

The next step is to decide the parts that will provide motion to the links. The **Motion** tab has a subcategory of motors which has an extensive list of options for specifying the type of motion provided by the motor. The motor can be controlled on the basis of Angle, angular acceleration, torque and RPM. The time vs Angular velocity graph can be imported or typed in manually. The use of controller for controlling the speed of the motor shaft can be turned on or off based on requirements. The two links or just a single link to which the motor is attached can be restrained motion to the centreline of shaft of motor motion.

8) Click on **Motion** and select **Motors.** Separate the joints using **Move** option and select the Link that needs to be given motion to in the first click and in the second click, the place where the motor is to be attached is selected. First select **ROBOTDESIGNPART2** and select the hole where the shaft of the motor will be used to control its motion. In the second click **ROBOTDESIGNPART2** is selected.

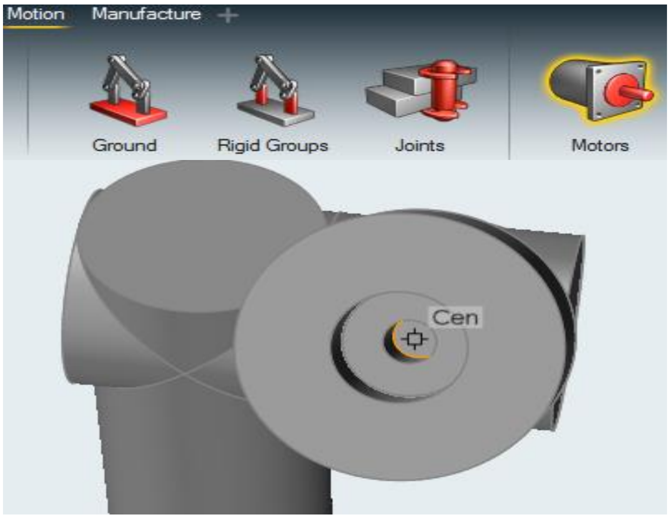

Figure 35 Fitting virtual motors in the design

9) Double click on the motor to further specify the details for the motor. On the left of the small tab that opens, set the motor motion to RPM and set the RPM as 15. Moving towards the right of the options on the tab select table and set it to step-dwell-step. This is the shaft speed profile that will be followed by the motor. On the next option to the right select option to edit the profile curve of the motor. In the profile editor tab that opens set the start time to 0 seconds and dwell time to 9, step on duration to 0.5 seconds, dwell time to 9 seconds and step off duration to 0.5 seconds. Untick the **use controller** option and select the **restrain centreline** option. Repeat the same process for every link joint and set the same profile for every motor. The motors are attached between **ROBOTDESIGN6PART2** and **ROBOTDESIGN6PART3, ROBOTDESIGN6PART4** and **ROBOTDESIGN6PART3, ROBOTDESIGN6PART5** and **ROBOTDESIGN6PART4.**

The direction of gravity has to be specified before analysis of the model as it plays a major role in deciding various factors during kinematic motion.

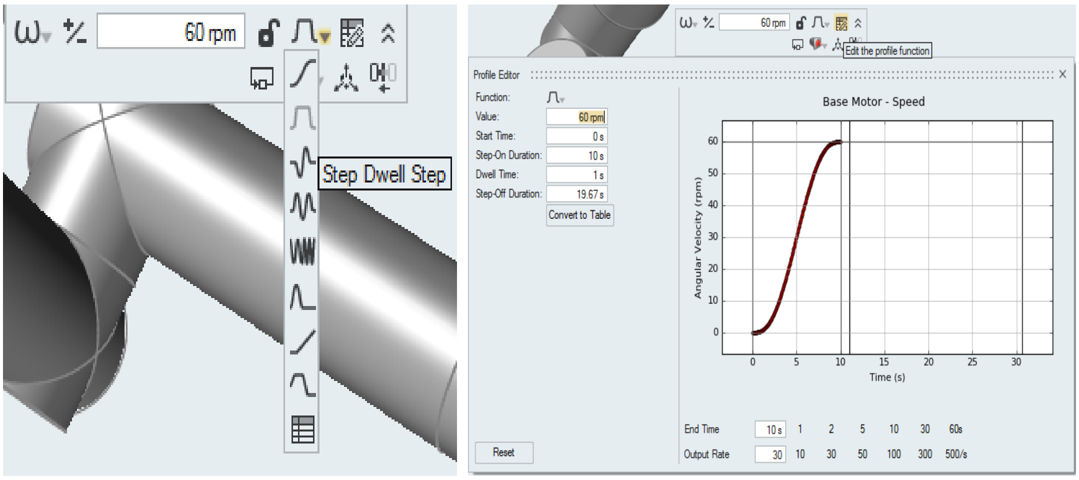

Figure 36 Defining motor specifications

10) Under the **Motion** tab select **Gravity** and make sure the arrow is pointing downward to the **ROBOTDESIGN6PART1** which is the base of the robot. Click on the arrow to reverse the direction and in the small tab that opens up, specify the direction in which gravity has to act.

The arm is planned for picking a weight of 1kg.

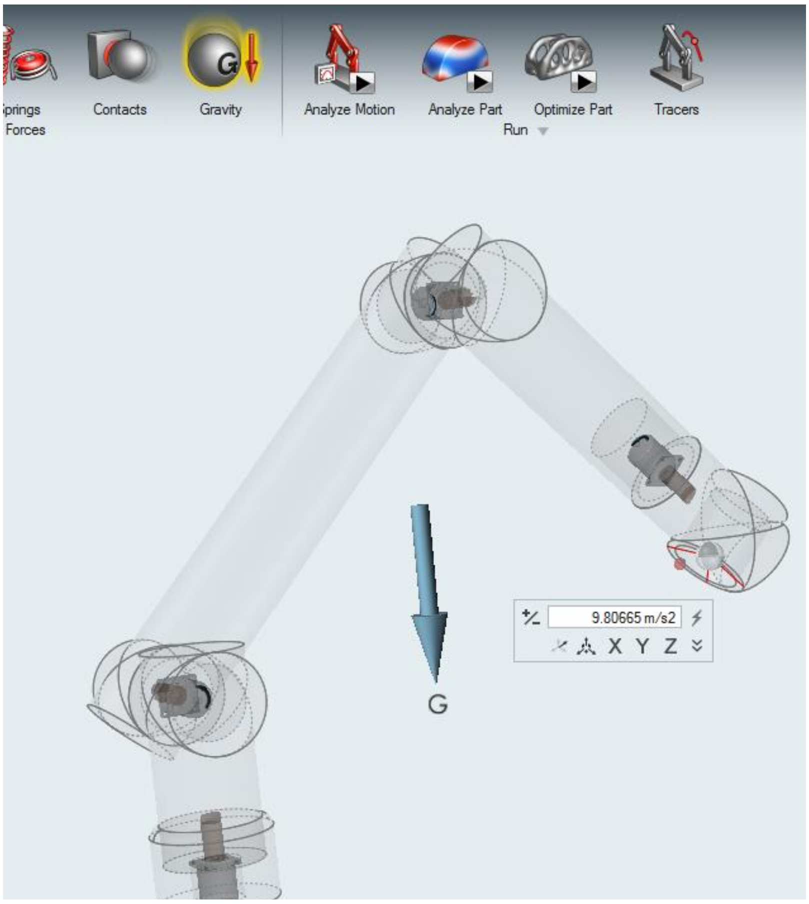

Figure 37 Considering Centre Of Gravity of the design

11) Under the **Structure** column click **masses** and set attach the mass to the end of **ROBOTDESIGN6PART5** and set it to 1kg and rigid in the small tab that opens.

Tracers can further be used to view the path which the end effector follows to understand the workspace of the robot.

12) Under **Motion** tab click on **Tracers** and attach it to the end of **ROBOTDESIGN6PART5.**

Figure 38 Adding Tracer Points

Analyze Motion option is used to run the model and see the effects in real time. The time for which the calculations are to be carried out are specified in the end time. The options to include Gravity, Contacts and many more are available in this category.

13) Under the same tab **Motion,** move the mouse to **Analyze Motion** and click on the chart that appears on the lower right corner of the **Analyze Motion** icon. Set the end time and Output rate to the desired level of required accuracy and time constraints. Click on

Figure 40 Fixing mass at a point

Figure 39 solving motion analysis tool

the play button on moving the mouse to Analyze Motion button

The calculations are carried out with information being retained at every instant specified in the **Analyze Motion** option.

4.2 First Design Layout

Figure 43 Structure of Design 1

The structure shown in Figure-42 is formulated with the theoretical idea that the link movement should not interfere with each other. The design allows 360 degree of motion for all links without interference with other links and also on the base level. But this design has a major flaw

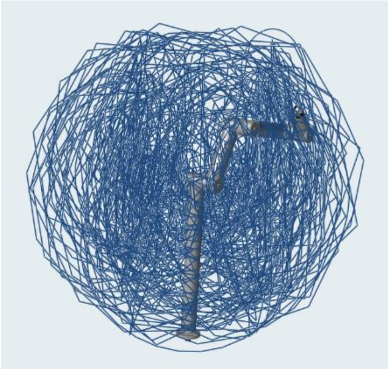

Figure 42 Workspace (Front View)

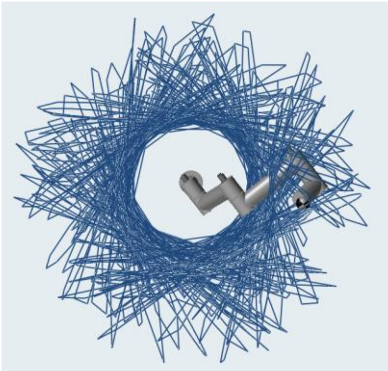

Figure 41 Workspace (Top View)

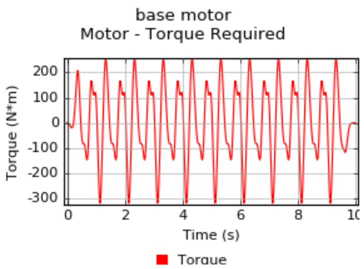

Figure 47 Base motor torque analysis

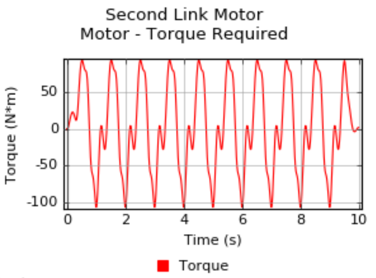

Figure 45 Second link motor torque analysis

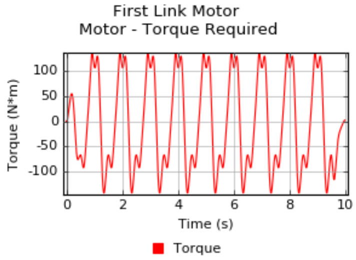

Figure 46 First link motor torque analysis

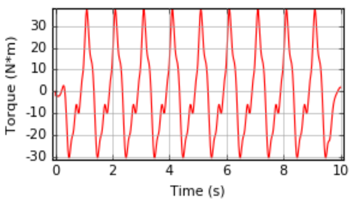

Figure 44 End effector motor torque analysis

Referring Figure-41 and analyzing the tracing point it is inferred that the end effector does not reach anywhere on the level of the base. The workspace sphere is centered around the first joint of the robot. From Figure-40 it is inferred that the end effector cannot reach any point around the volume of the base which forms a cylindrical unreachable workspace. The design does not accomplish the task. The motor also requires a huge amount of torque. From Figure-46,45,44 it is inferred that the torque requirement is well above 300 Nm for the base motor and the two motors require about 150 Nm. The design is completely inefficient.

4.3 Second Design Layout

The second iteration of the design is close to the arrangement in Figure-49. Inferring from figures Figure-47 and Figure-48; the workspace sphere is formed around the first joint. The End effector is capable of reaching the base level. But its collision with the ground is unavoidable as inferred from the first design. The workspace volume around the base of the robot has also increased.

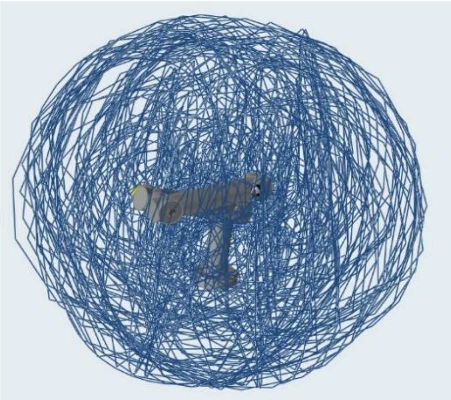

Figure 48 Workspace Area (Front view)

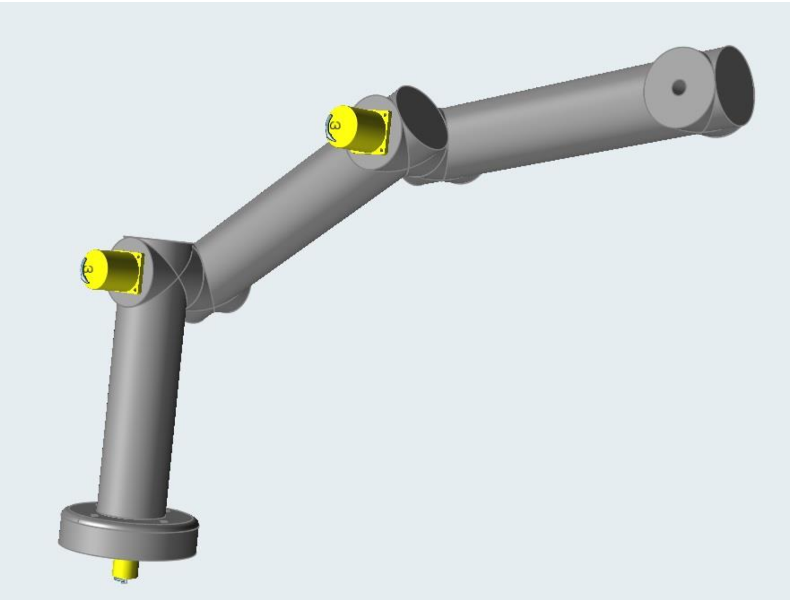

Figure 50 Structure of Design 2

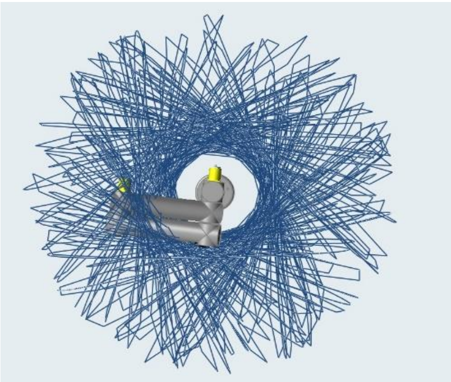

Figure 49 Workspace Area(Top View)

Also comparing the torque analysis of first and second design motors (Figure-50,51,52,43,44,45,46) it is clear that torque requirement for the second design is lower and thus more efficient. But this design does not incorporate the motor within the design itself.

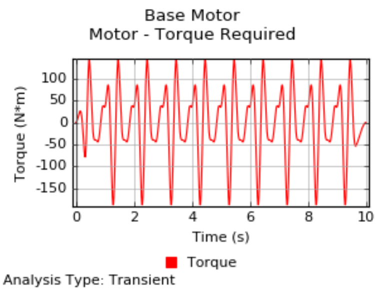

Figure 51 Base motor torque analysis

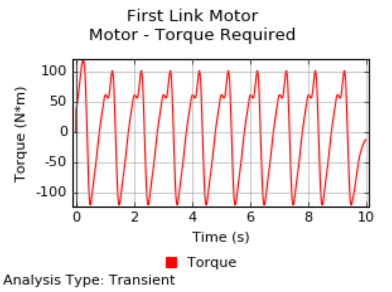

Figure 52 First link motor torque analysis

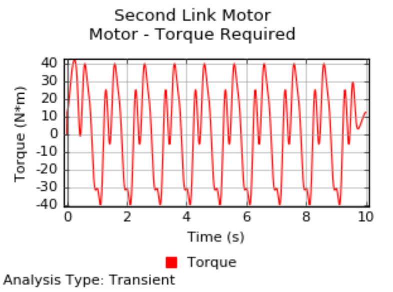

Figure 53 Second link motor torque analysis

.

4.4 Third Design Layout

Figure 54 Structure of Design 3

Referring **Fig 53**, the motors have been incorporated inside the link arrangement itself. Housing for the motor is cylindrical inside the link arrangement. The link movement will not be hindered with the presence of protruding motors.

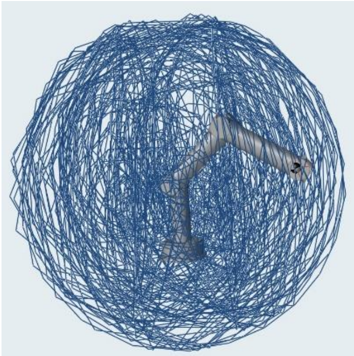

Figure 59 Workspace (Front view)

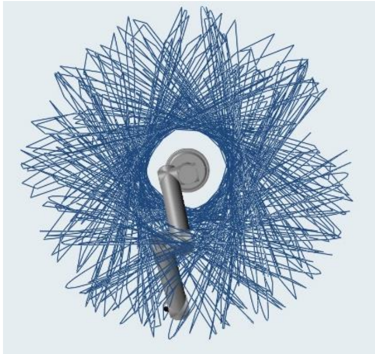

Figure 58 Workspace (Top View)

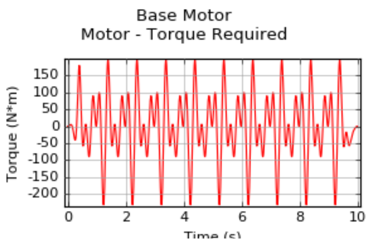

Figure 57 Base motor torque analysis

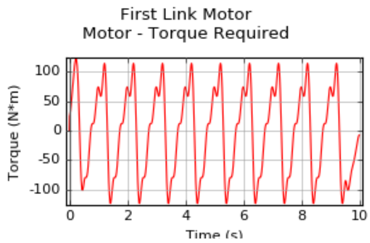

Figure 56 First link motor torque analysis

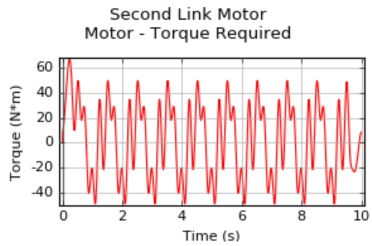

Figure 55 Second link motor torque analysis

For reach near the workspace another degree of freedom had to be introduced to provide one more angle for the end effector approach angle. The torque required had to be reduced.

4.5 Fourth Design Layout

This design adds up one more degree of freedom providing an extra angle for the end effector approach. Link number 3 has been divided in 2 parts with a planar joint in between the two. This arrangement increases the dexterous workspace of the robot significantly. The reach of the end effector increases drastically as we can see from **Fig 59** and **Fig 60.**

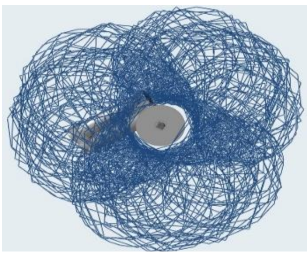

Figure 60 Workspace (Top View)

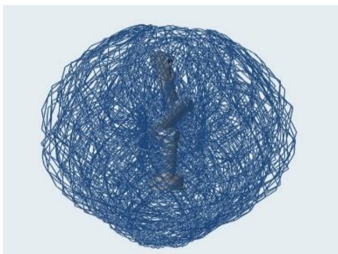

Figure 61 Workspace (Front View)

Figure 63 Structure of Design 4

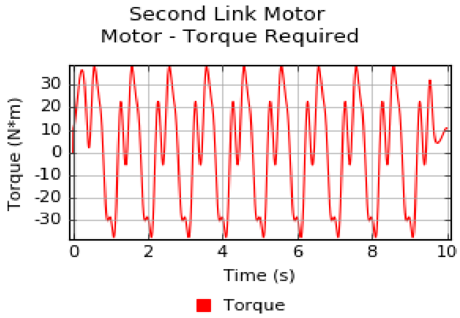

Figure 64 Second link motor torque analysis

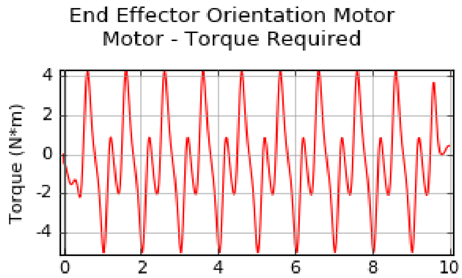

Figure 62 End effector orientation motor torque analysis

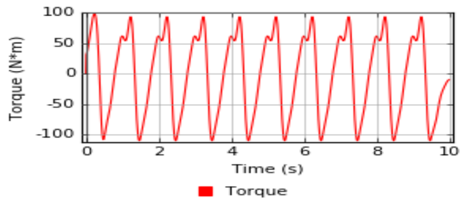

Figure 65 First link motor torque analysis

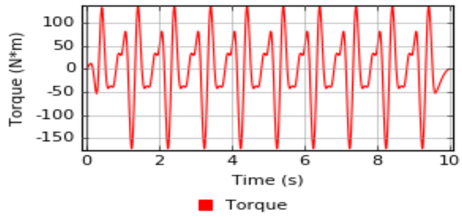

Figure 66 Base motor torque analysis

The end effector reach has been increased around the first link of the robot in comparison with the third design **Fig 59.** .
From figures **Fig 64** and **Fig 65** it is inferred that the torque requirement for the motors are approximately 170 Nm and 110 Nm respectively. These are relatively large values. To reduce the cost of the robot the torque requirement must be reduced. Hence we move on to fifth design layout.

4.6 Fifth Design Layout

This is the most efficient design of all the above designs. The length of the 1st link is reduced to half to increase the reach of the end effector which is visible in **Fig 66.** There is no space left out around the first link compared to design 4 from **Fig 68**. The link arrangement has been altered to increase the efficiency of motors and thus requiring less torque. The length of the second link is increased from the fourth design iteration and the third and fourth have been decreased to help it move around freely without hindrance from the first link.

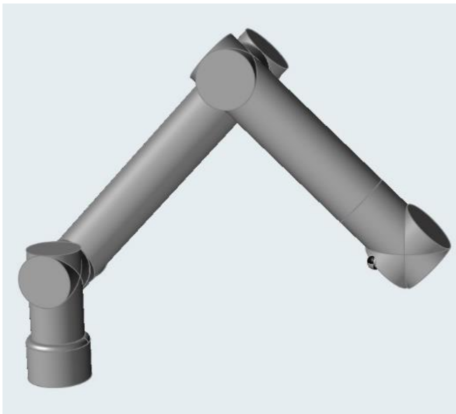

Figure 67 Structure of Design 5

The workspace sphere is formed about the first joint and it is obvious that the reach on the base level will be more with this design.

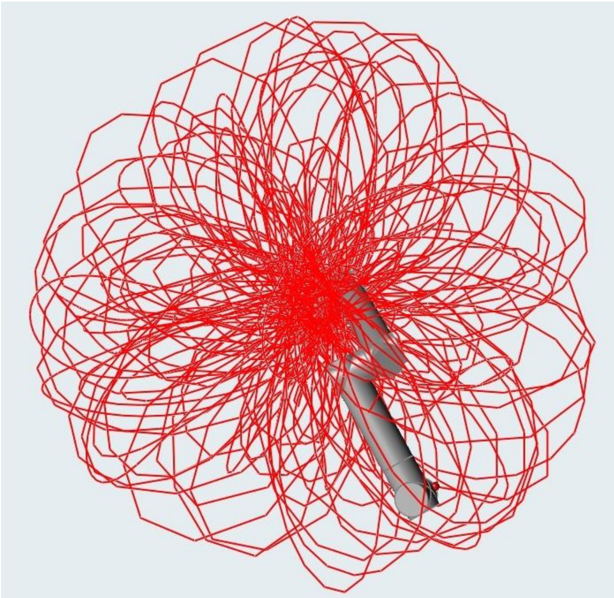

Figure 68 Workspace (Top View)

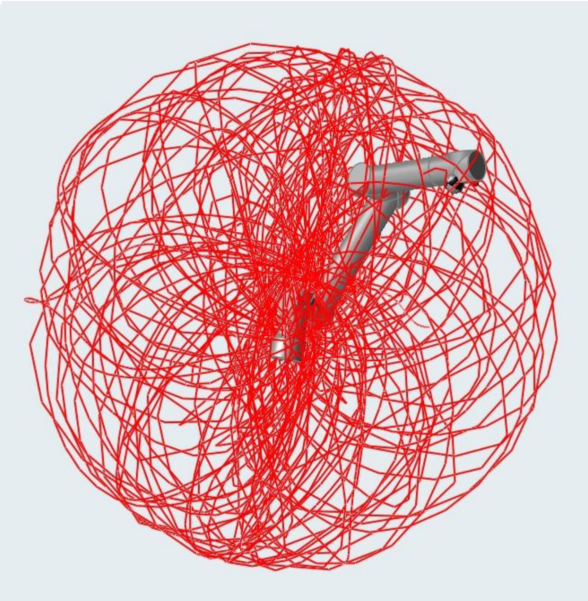

Figure 69 Workspace (Front View)

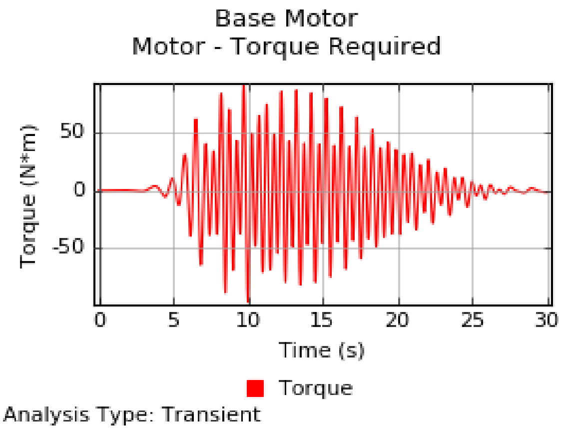

Figure 71 Base motor torque analysis

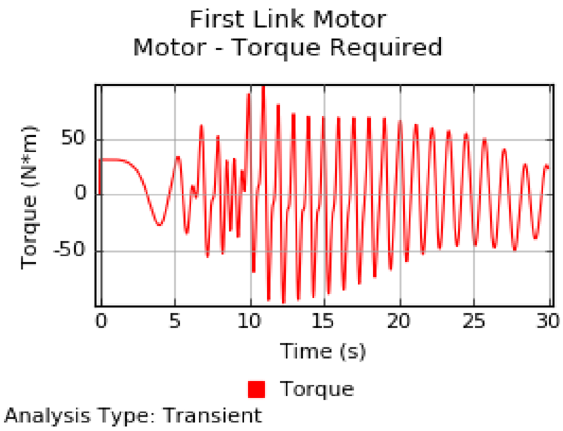

Figure 70 First link motor torque analysis

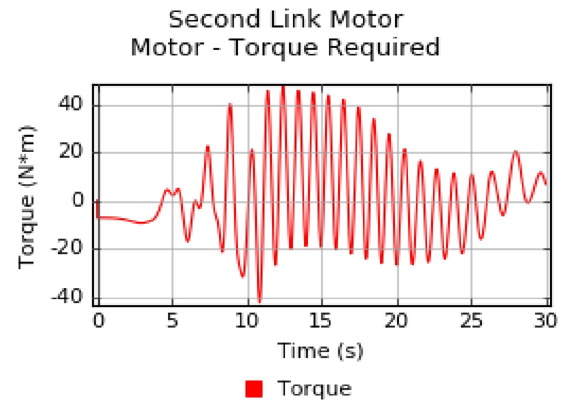

Figure 73 Second link motor torque analysis

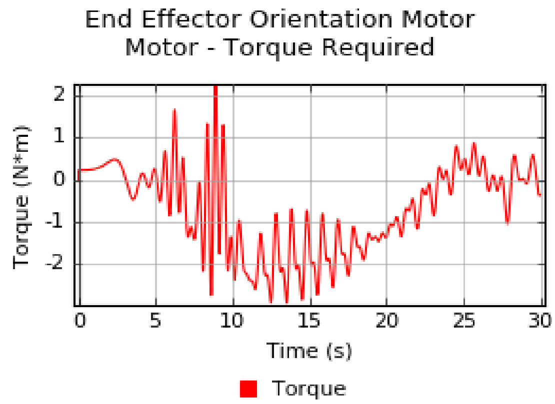

Figure 72 End effector orientation motor torque analysis

Table 3 Percentage Reduction in Required Torque

Motor	Percentage Reduction With Each Generation (%)				
	Design 1	Design 2	Design 3	Design 4	Design 5
Base Motor	-	50	-46	23	42
First link motor	-	30	0	0	34
Second link motor	-	60	-37	43	-22
End effector orientation motor	-	-	-	-	50

Comparing the torque required in design 4 with design 5 it is inferred that there has been a reduction of about 90 Nm for the base motor (**Fig 70** and **Fig 63**) and 30 Nm approximately for the first link motor (**Fig 69** and **Fig 62**).

The power required is lower, the dexterous workspace is greater. Thus this is the most efficient design of all the five designs. The design specifications are mentioned in the forthcoming figures.

4.7 Degree of Freedom of the final design

The final design structure's degree of freedom will be determine using the Grubler's equation. (**Give Reference).** The final design's orthographic projection is given in the figure below:

Using the **Grubler's formula:** (Equation 4) .

$$\boldsymbol{Degree\ of\ freedom} = \boldsymbol{m(N-1-J)} + \sum_{\boldsymbol{i=1}}^{\boldsymbol{J}} \boldsymbol{f_i}$$

Equation 4 Grubler's formula

the degree of freedom of the whole structure can be determined.

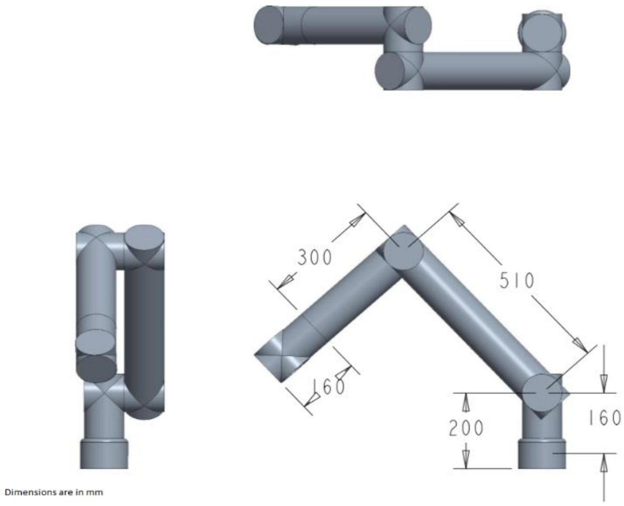

Figure 74 CAD model of assembled design 5

Variables in the Grubler's equation:

Defining "m" for the structure: The degree of freedom of a rigid body in space is mentioned using **"m".** For any rigid body the degree of freedom is 6. Hence the value of **"m"** is 6. *(Figure 74-75)*

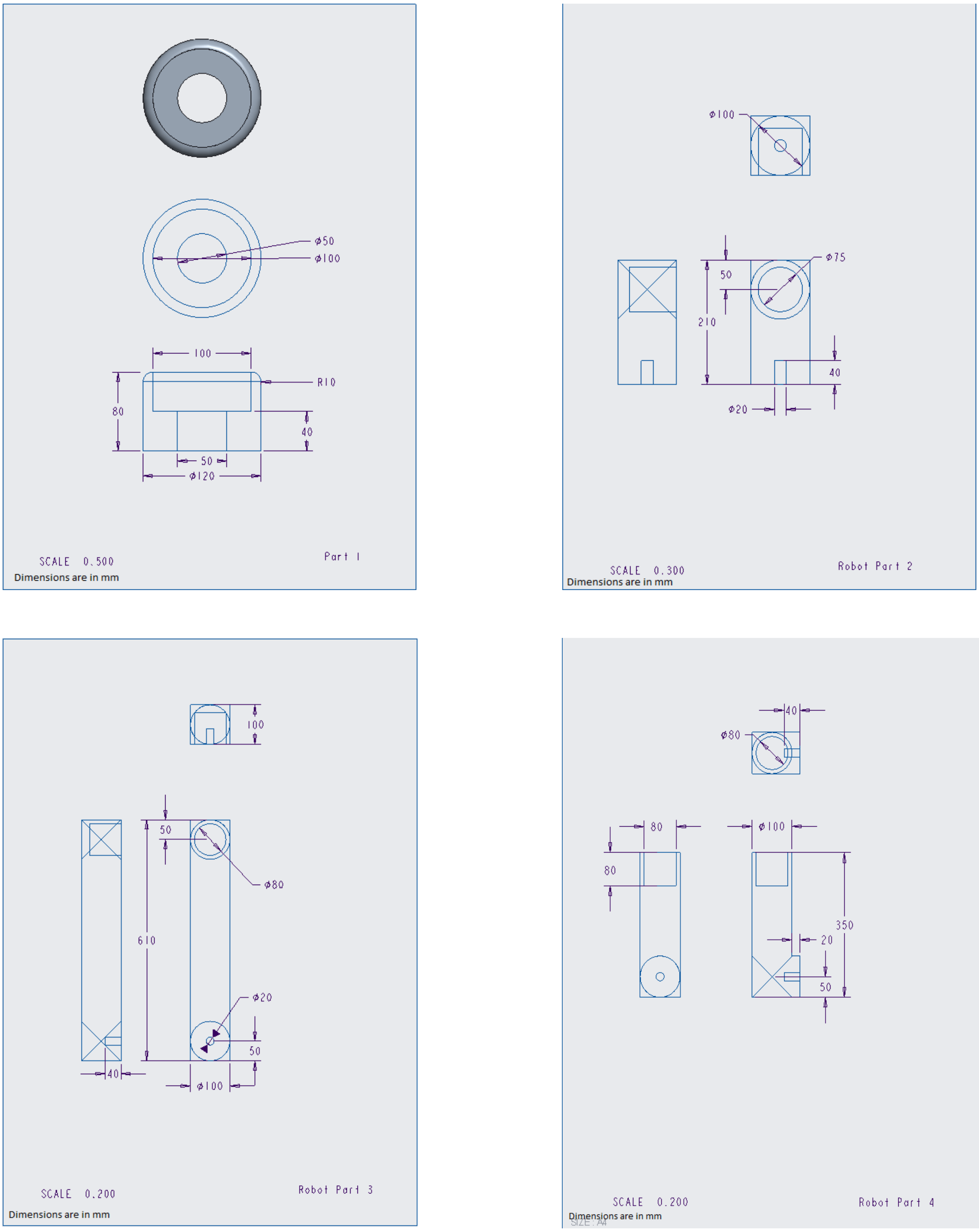

Figure 75 Parts of design 5

Defining "N" for the structure:

"N" is the number of rigid links included in the structure. It also takes into account the grounded parts.

The individual links of the structure's orthographic projection is included in the figures below:

There are 5 rigid links in the structure. *(Figure 74-75)*

Hence **N = 5.**

Defining "J" for the structure:

"J" is the number of joints included in the linkage.

The types of joints in the structure are

1. **Twisting Joint**
2. **Revolute Joint**

1. **Twisting Joint:**

There are **2** twisting joints included in the structure.

The joint between **Part 1***(Figure 74)* and **Part 2** *(Figure 74)*

The joint between **Part 5***(Figure 75)* and **Part 4***(Figure 74)*

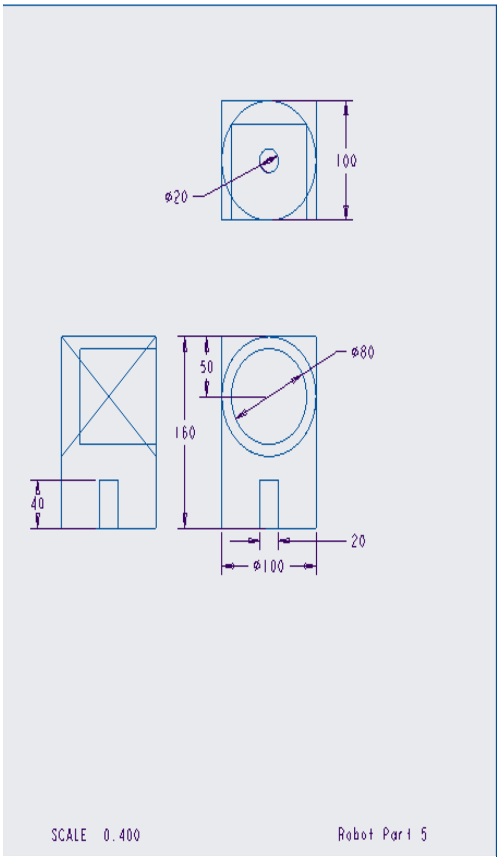

Figure 76 Part 5 Design 5

2. **Revolute Joint:**
   There are **2** revolute joints included in the structure.

The joint between **Part 2***(Figure 74)* and **Part 3** *(Figure 74)*

The joint between **Part 3***(Figure 74)* and **Part 4** *(Figure 74)*

Hence the value of "**J**" is the sum of 2 twisting joints and 2 rotary joints. **J = 4**.

Giving joint number to each of the joints

Table 4 Joint naming

JOINT	LINKAGE
1	PART 1 & PART 2
2	PART 2 & PART 3
3	PART 3 & PART 4
4	PART 4 & PART 5

Defining "f_i" for the structure:

f_i is the degree of freedom of i^{th} joint. Each type of joint has its own degree of freedom.

Degree of freedom of Twisting joint:

The Twisting Joint has 1 degree of freedom. The ouput axis is aligned with the input axis and rotates around it.

Degree of freedom of Revolute joint:

The degree of freedom of a revolute joint is 1. There is only 1 type of motion that is possible between the 2 rigid links connected by a revolute joint.

Table 5 Types Joints used and their degree of freedom

Joint	Degree of freedom
Twisting Joint	1
Revolute Joint	1

Now, calculating the value of "$\sum f_i$"

Table 6 Joint name and their degree of freedom

f_i	Joint	Degree of freedom
1	1	1
2	2	1
3	3	1
4	4	1

$$\sum f_i = f_1 + f_2 + f_3 + f_4$$

$$f_i = 4$$

Using all the values in the equation:

$$Degree\ of\ freedom = m(N-1-J) + \sum_{i=1}^{J} f_i$$

Degree of Freedom = 6(5 - 1 – 4) + 4

Degree of Freedom = 6(0) + 4

Degree of Freedom = 4

The Degree of freedom of the structure is found to be **4**.

4.8 Defining the joints

The next step in the design process is defining the joints that will connect the links and allow motion. Motion will be provided to the links with the help of stepper motors. The torque requirement from the motion analysis obtained from the basic draft of the design layout is very large and quite unrealistic due to two main reasons

- *The material into consideration while performing the motion analysis:*
  A lot of unnecessary materials are included in the design hence increasing the weight of each link considerably thus increasing the torque requirement.
- *Direct motion transmission from motor to link:*
  The method for connecting the links with each other has to be defined with practicality. The shaft of the motor cannot bear the weight of their links and the links succeeding them. The torque transmission capability of the motor to the link has to be increased as well. Stepper motors with large torque transmission capability are quite large/heavy and cannot be included in the robot design. Hence the torque provided by the small sized stepper motors have to be multiplied by some mechanism.

For defining the joints and the method of linkage between the links gears seem to be the best solution.

5 Gears

5.1 Introduction

Some main advantages of using gears are:

1. **Torque Multiplication** .
   The number of teeth on each gear decides the torque output. A specific gear set will have a gear ratio. If the gear ratio is 5:1 then the input of a 1 Nm will provide an output of 5 Nm.

2. **Speed Reduction**
   A vast range of stepper or servo motors do not operate efficiently on low RPM. The planetary gear system not only multiplies the torque but as a result it has to trade in with speed which is a win-win situation as intended with operation at intended RPM and voltage of the motors.

3. **Inertia Matching**
   A high initial load inertia compared to the initial load inertia of the motor then there is an excessive overshoot or increased settling time. To solve this higher torque motors can be used but for most of the running time the potential of such motors is wasted and there is a lot of wasted power. In such cases, a gear set can help match the initial load inertia with the motor inertia creating a more efficient and responsive system.

4. **Cost Savings** .
   Getting a higher torque, reduced speed and increased response times are all beneficial and thus will require smaller motors, drives and overall reduced power usage.

There are various types of gears to choose for the application in robotic joints. These are the main types of gears:

1. **Spur Gears**: They are the most commonly used gears. The gears are arranged in parallel to the shaft. The teeth on the spur gears are parallel to the shaft axis, the result being production of radial loads on the shaft without any axial loads. They tend to be noisy during operation because of a single point of contact between the teeth.

Figure 77 Spur Gear

2. **Helical Gears**: They are almost similar to the spur gears in operation. The only difference being the angle at which the tooth of the helical gears are arranged in respect the shaft axis. They are aligned at an angle because of which there is more than one point of contact during meshing leading to smoother and quieter operations .

Figure 79 Helical Gear

3. **Bevel Gears:** They are used in applications where power transmission is required between shafts inclined at 90 degrees with each other .

Figure 78 Bevel Gear

4. **Worm Gear:** They are used in non-intersecting shafts. A screw shape is cut on the shaft called the worm and the mating gear is the worm wheel. They produce a thrust load and are good for high shock load applications but offer lower efficiency.

Figure 80 Worm Gear

For design of the prototype industrial robot the spur gears will be used.

5.2 Gear Terminology

Some basic spur gear terminology which will be used for design of the spur gears are as follows.

Addendum: this is an imaginary circle through the outermost face of the tooth throughout the gear

Dedendum: This is an imaginary circle through the root of the tooth.

Base Circle: This is the circle through which the involute profile of the spur gear is generated.

Pitch circle: This is an imaginary circle where the point of contact always lies when gears mesh with each other or in other words it is a circle formed by extending the pitch point throughout the circle

Diametral pitch: This is the ratio of number of teeth with the pitch circle diameter or in other words it is the teeth per millimeter of pitch circle diameter

Pitch Diameter: It is the ratio of number of teeth to the diametral pitch

Module: It is the ratio of pitch circle diameter to the number of teeth

Line of action: It is the line along which the meshing contact point of gears takes place from one end to the other. It means that the point of contact between the gears travels through the line of action

Pressure angle: It is the angle formed between the line perpendicular to the line of line of centers and the Line of action

Clearance: It is the distance between the bottom of one gear to the top face of the meshing gear

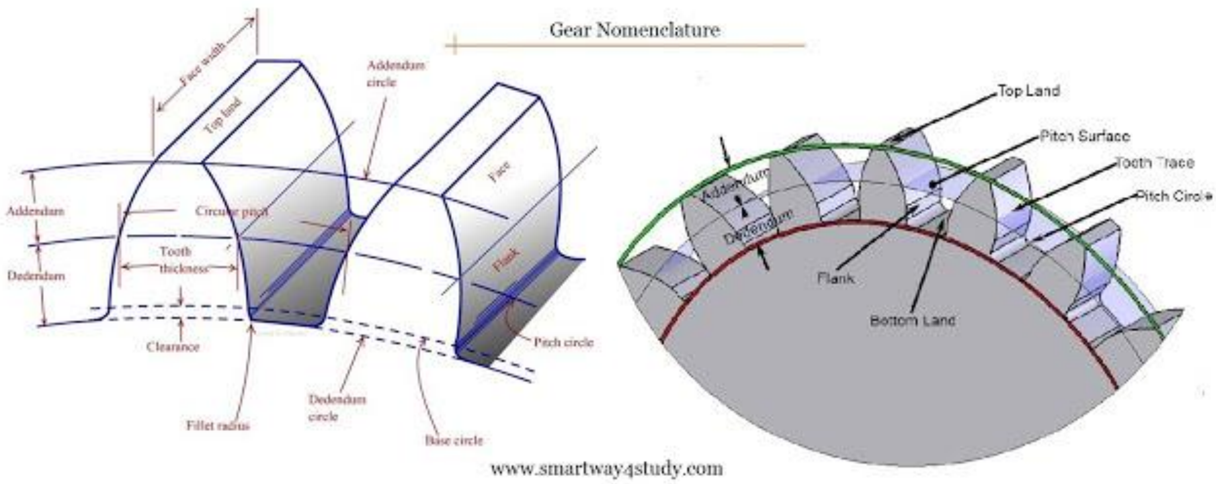

Figure 81 Spur Gear Terminology

5.3 Gear Ratios:

For gears to mesh it is absolutely necessary that at the point of meshing the velocity of each gear must be equal. If not then one gear would slip with respect to the other at the point of contact. The gear ratio formula is derived from this concept.

If v_1 & v_2 are the velocities of 1 and 2 gears that are in mesh, then

$$v_1 = v_2$$

We know that $v = \omega * r$ where r is the radius of the pitch circle. Then

$$\omega_1 r_1 = \omega_2 r_2$$

As the gear ratio is the ratio of angular velocities then

$$Gear\ Ratio = \frac{\omega_1}{\omega_2} = \frac{r_2}{r_1}$$

Equation 5 Gear Ratio

Also

Number of teeth = z

Module = m

Pitch circle diameter (d_p) = m*z

For meshing gears we know that the module must be equal, hence

$$m_1 = m_2$$

$$\frac{d_1}{z_1} = \frac{d_2}{z_2}$$

$$\frac{z_2}{z_1} = \frac{d_2}{d_1} = \frac{2r_2}{2r_1} = \frac{r_2}{r_1}$$

Equation 6 Gear Ratio

5.4 The Planetary Gear System:

This is nothing but a set of compound gears used together in operation. It provides very gear ratios in small spaces. This is ideal for the design and fabrication requirements of the robot.

There are 3 types of gears in this system

- Sun gear
- Planet Gear
- Ring gear

The main constraint for the size and number of teeth will be the size of the joint itself in which the whole planetary gear set will be incorporated.

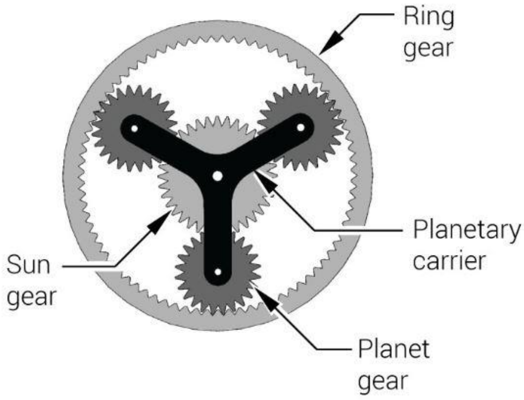

Figure 82 Planetary Gear System

The pitch circle diameter of the Ring gear must be within 85 mm diameter for extruding them within the joint itself. So the sun and planet gears must have dimensions such that they give the overall gear reduction ratio of the planetary gear system to be 4 or more. The dimensions of the sun and planet gears will be decided on the basis of the gear ratio of the planetary set.

Gear reduction ratio of planetary gear system derivation: [5]

Let subscripts *r, p, s* and *c* be used for ring gear, planetary gear, sun gear and planet carrier respectively.

Let r_r = Radius of ring gear

r_p = Radius of planet gear

r_s = Radius of sun gear

From figure number (Figure-82) it can be deduced that

$r_r = r_s + 2r_p$

$2r_p = r_r + r_s$

Equation 7 Epi-cyclic Gear Size Relationship

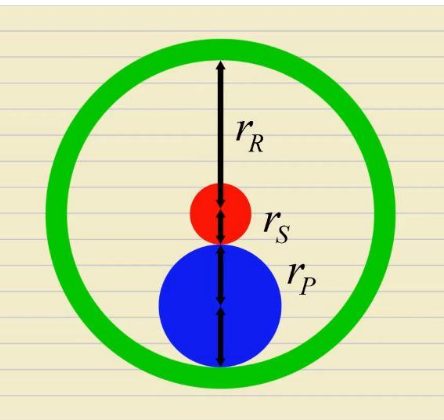

Figure 83 Gear Sizes

Also we know that planet carrier is attached to the center of the planet gear hence,

$r_c = r_s + r_p$

Equation 8 Epi-Cyclic Gear Size Relationship

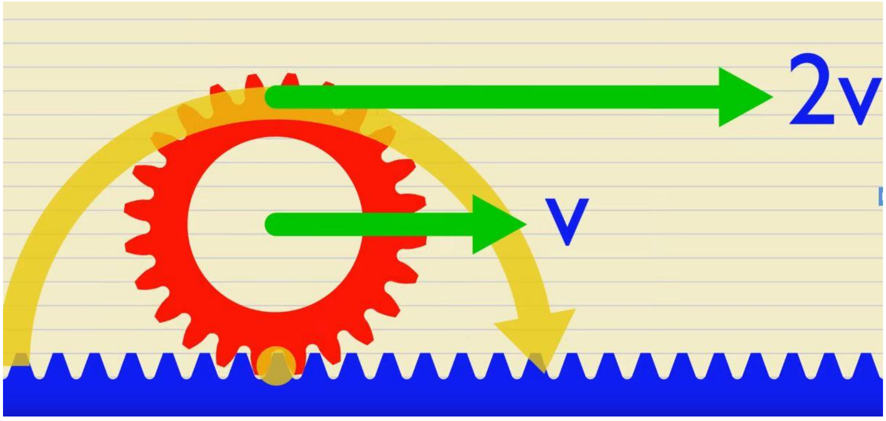

Figure 84 Gear Horizontal velocity

From Figure-83 we can deduce that the velocity at the top point of the red gear through the method of instantaneous centers. The instantaneous center is at the bottom meshing part of both the gears.

This velocity conditions also apply to the planetary gears in the planetary gear mechanism as shown in Figure-84

In the planetary gear system, the input will be to the sun gear and the output will be obtained from the planet carrier, hence from equation number Equation-5 we know that

Gear Ratio = $\frac{\omega_1}{\omega_2} = \frac{r_2}{r_1}$

From this we can write that

Gear Ratio = $\frac{\omega_s}{\omega_c}$

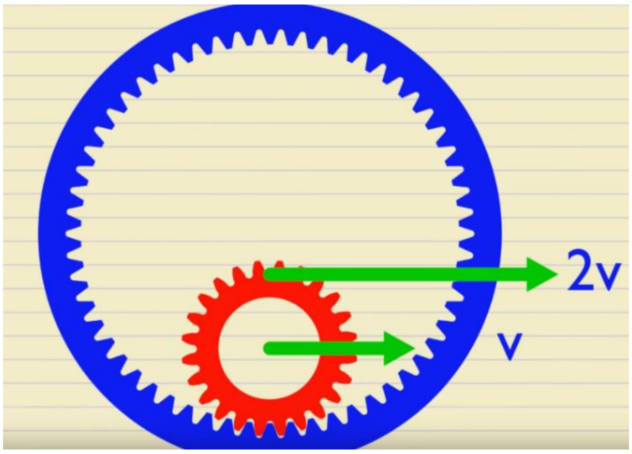

Figure 85 Gear Transverse Velocity

$v_c = \omega_c * r_c$

$v_c = \omega_c * (r_s + r_p)$ From Equation-8

$v_s = \omega_s * r_s$

We established that $v_s = 2 * v_c$ (Figure-85)

So,

$\omega_s * r_s = 2 * \omega_c * (r_s + r_p)$

$\frac{\omega_s}{\omega_c} = \frac{2(r_s + r_p)}{r_s}$

$\frac{\omega_s}{\omega_c} = \frac{2r_s + 2r_p}{r_s}$

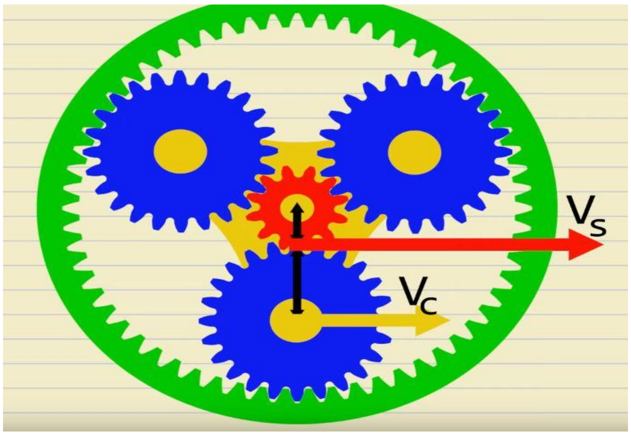

Figure 86 Gear Rotational Speed

$\frac{\omega_s}{\omega_c} = \frac{2r_s + r_r - r_s}{r_s}$ From Equation-7

$\frac{\omega_s}{\omega_c} = \frac{r_r + r_s}{r_s}$

$\frac{\omega_s}{\omega_c} = 1 + \frac{r_r}{r_s}$

$\frac{\omega_s}{\omega_c} = 1 + \frac{z_r}{z_s}$ From Equation-6

Equation 9 Epi-Cyclic Gear Ratio

5.5 Finalizing Gear Parameters for Joints

From Equation-6 it is obvious that by increasing the number of teeth on the ring gear and keeping the number of teeth on sun gear as low as possible, we can attain a high gear ratio.

Diametral Pitch:

For maximum number of possible teeth on a gear, the diamteral pitch needs to be 1.

Sun gear:

For avoiding any size and strength constraints, the pitch circle diameter of the sun gear is finalized at 16 mm. As the diametral pitch is kept 1, the number of teeth on the sun gear will be 16.

$$d_p = \frac{z_s}{d_s} \; (d_s = \text{pitch circle diameter of the sun gear})$$

$$1 = \frac{z_s}{16}$$

Ring gear:

The diameter of the link is not to exceed 100mm. The joint must be within this range. For some allowance between the joint and the outmost link surface, the pitch circle diameter of the ring gear is fixed at 80mm.So the number of teeth on the ring gear will also be 80.

$$d_p = \frac{z_r}{d_r} \; (d_r = \text{pitch circle diameter of the ring gear}).$$

$$1 = \frac{z_r}{80}$$

Planet Gear:

The diameter of the planet gear can be calculated by subtracting the radius of ring gear with the radius of the sun gear

$$2r_p = (d_r/2) - (d_s/2)$$

$$2r_p = (80/2) - (16/2)$$

$$2r_p = 40 - 8$$

$$2r_p = 32$$

The diameter of planet gear is found to be 32mm.

The dimensions of all the gears have been decided.

5.6 Methodology of designing the gears. [5]

The teeth profile of the spur gears are created from the involute of a circle. An involute of a circle is that path of curve traced from the end of a wire wound around a circle when unwounded keeping the string taut as seen in Figure-87. The red line traced is called the involute of a circle. This involute profile forms the shape for the profile of the tooth in spur gears. In gears the involute profile is traced for the base circle diameter.

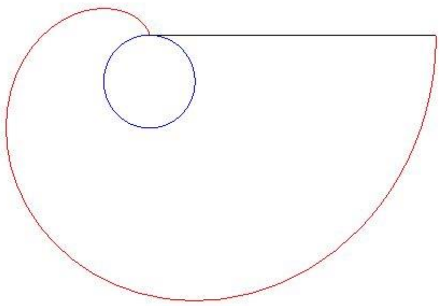

Figure 88 Involute Profile Of A Circle

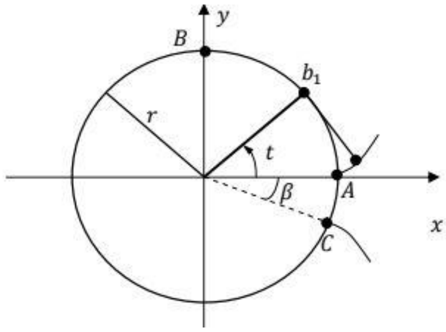

Figure 87 Involute Profile For Designing Gear

Referring Figure-88, the involute profile have been traced at two different points. The angle between the traced Involute profiles *Inv1* and *Inv2* on the base circle have to be found for creating the gear profile.

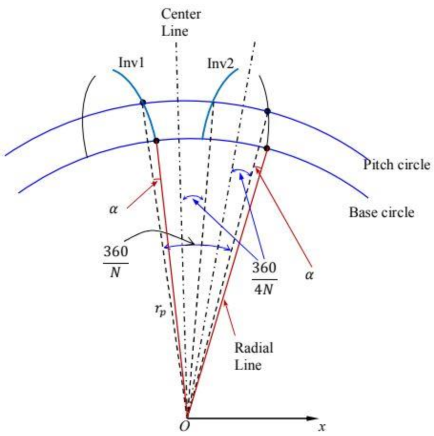

Figure 89 Teeth Deigning

The angle between the same points on the adjacent teeth is $\frac{360}{N}$ if N is the total number of teeth. Upon dividing this angle into 4 equal parts, the angle subtended will be $\frac{360}{4N}$.

In Figure-88 it can be seen that by subtracting $\frac{360}{4N}$ by α, we will get half the value of the angle subtended by the two involute profiles from the base of the circle. Let us name it β.

α = $\frac{\sqrt{d_p^2 + d_b^2}}{d_b} - \phi$ (d_p = diameter of pitch circle, d_b = diameter of base circle , ϕ = Pressure

$$\beta = \frac{360}{4N} - \alpha$$

Equation 10 Relation For Generating Tooth Profile

Therefore 2β will be the angle between *Inv1* and *Inv2* on the base circle. This angle is further used to create gears in CAD modelling. **[6]**

5.7 Gear Design in CREO

The above formulas and methods are used in designing the gears. In CREO Parametric.

Initial relations and parameters required:

To begin with the design process 3 initial parameters are defined based on which the rest of the gear relations can be derived.

Initial Parameters:

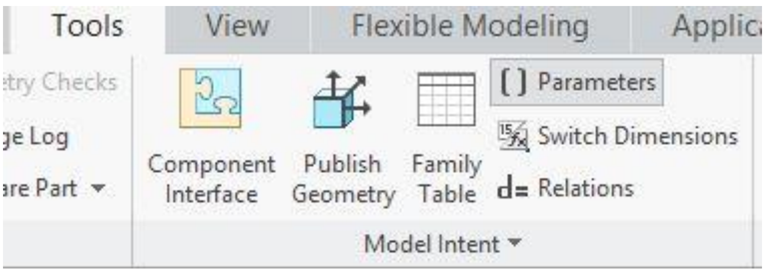

Figure 90 Parameter Tool

The initial parameters are uploaded in the **Parameters** section which is found under **Tools**. (Figure-89)

3 initial parameters that will be defined are

1) Diametral Pitch (P)
2) Number of teeth (N)
3) Pressure Angle (PHI)

Name	Type	Value
P	Real Numb	1.000000
N	Integer	16
PHI	Real Numb	20.000000

Figure 91 Defining Initial Parameters

An example is shown in Figure-90

Derived Parameters:

The relations used to derive the rest of the gear dimensions is:

A = 1/ P(addendum)

B = 1.25/P (dedendum)

C = B - A (clearance)

DP = N/P (pitch circle diameter)

DB = DP*cos(20) (base circle diameter)

AC = DP+(2*A) (addendum circle)

BC = DP - (2*B) (dedendum circle)

D0 = AC

They are entered in the **Relations** section found in **Tools** (Figure-91)

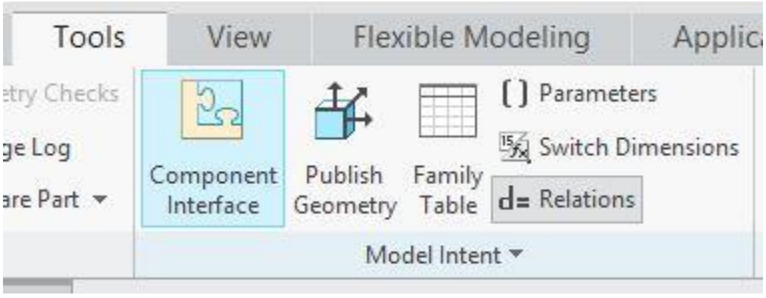

Figure 92 Relations Tool

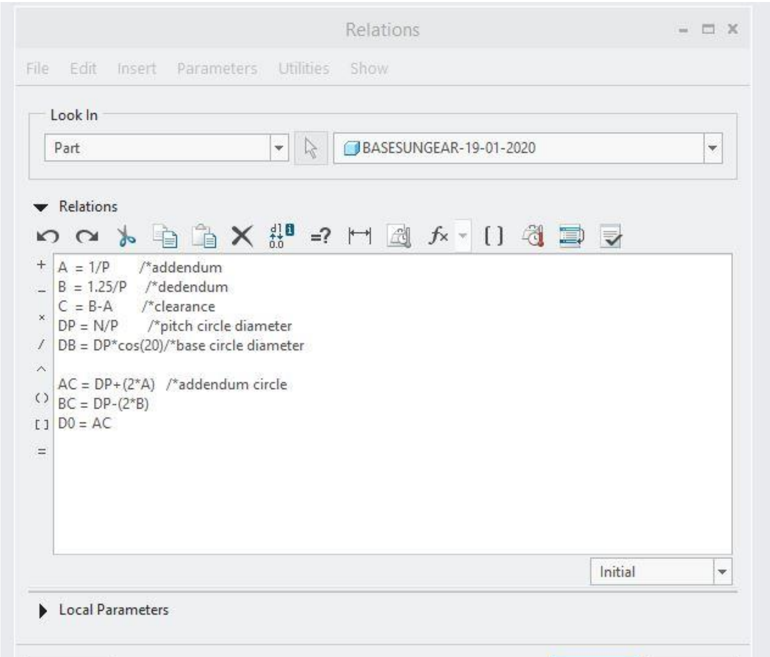

Figure 93 Defining Relations Using Relation Tool

All the terms used in the relations are used to decide the dimensions at each step. The addendum circle for example, the term used is **AC** which is already found using the relations. To initialize the value of **AC** and use it in the gear design step as shown in (Figure-93) '**AC**' is entered and the dimension is set accordingly based on the calculated values. Every

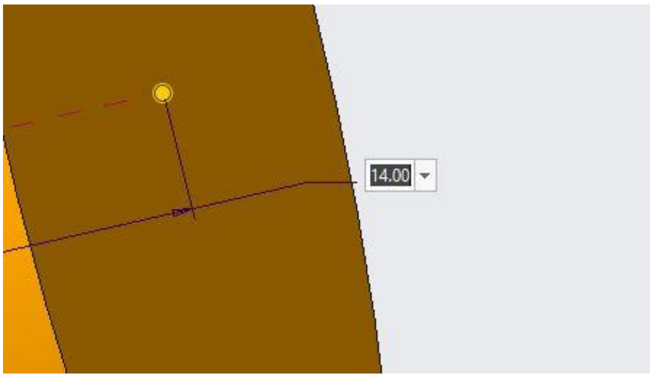

Figure 94 Initializing Addendum Circle

Every parameter can be defined in this manner. The Sun Gear, Planet Gear and also the Ring Gear can be designed using the methodology discussed in **Section 5.6**

Table 7 Specifications Of The Gears

Gear Type	**P (Diametral Pitch)**	**N (Number of Teeth)**	**PHI (Pressure Angle)**
Sun Gear	1	16	20°
Planet Gear	1	32	20°
Ring Gear	1	80	20°

General Steps to be followed for the gear design:

1) Define all the parameters mentioned in ***Section 5.7.*** The dimensions to be included are mentioned in **Section 5.5** for each gear.
2) Select any plane and sketch 4 circles on the plane
3) Edit the dimensions of each circle. In the edit dimensions box (Figure-93) type in '*AC*', '*BC*', '*DB*' and '*DP*' for each of the circles which are the addendum circle diameter, dedendum circle diameter, base circle diameter and pitch circle diameter respectively.
4) Extrude the '*AC*' or the addendum circle to 16mm.
5) Generate Involute profile of the base circle '*DB*' using the '*Generate Curve from Equation* option in CREO. (Figure-94)

5.1) On selecting the option ***Equation,*** a dialogue box opens (Figure-95)

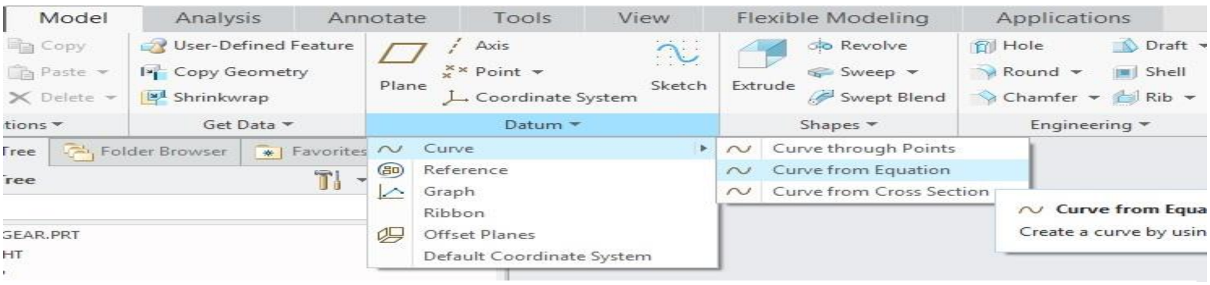

Figure 95 Generating Profile Of Teeth Using Curve From Equation

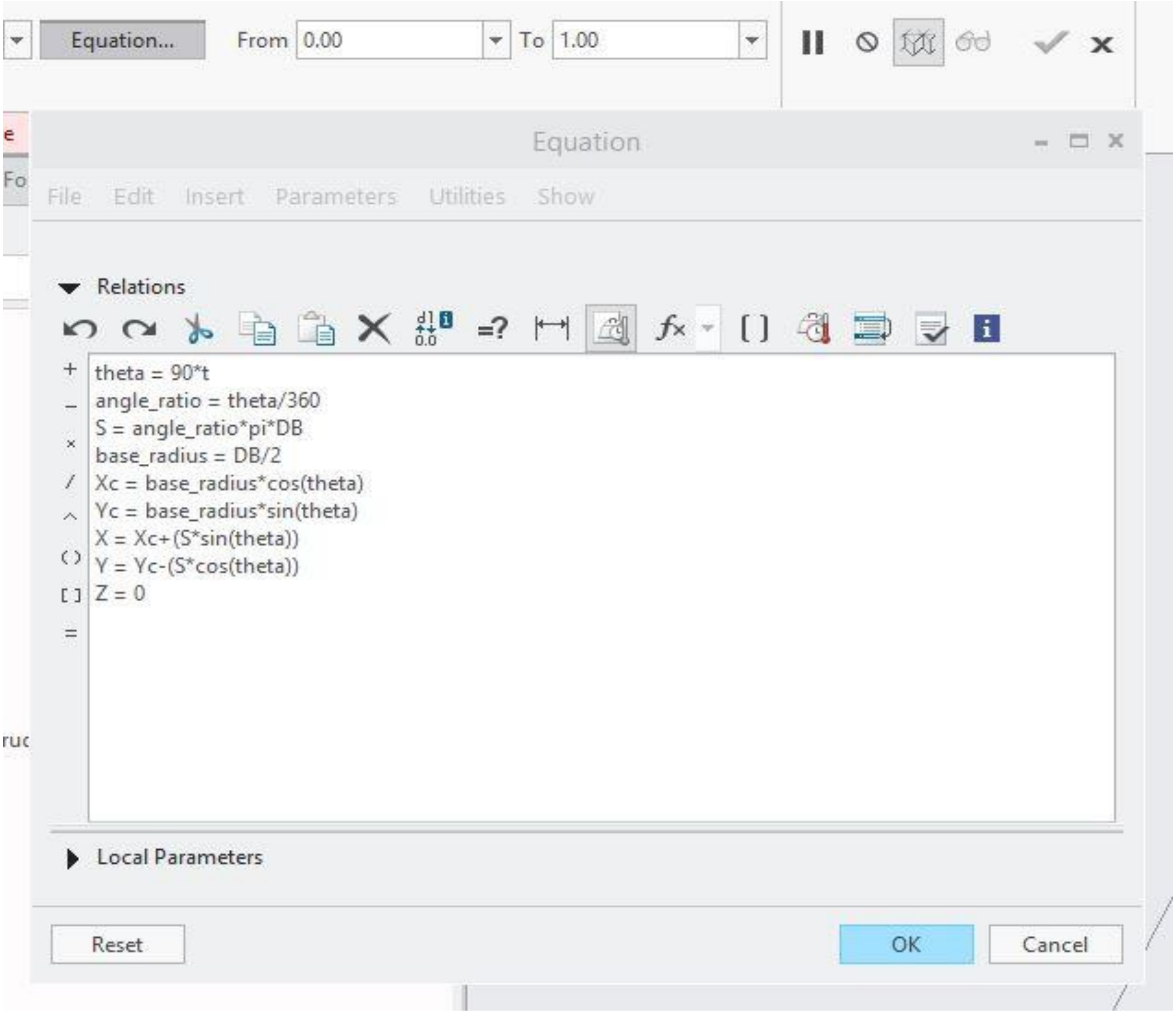

Figure 96 Dialogue Box Of Equation Tool

The equations to be entered for generating an involute profile of the circle are as follows:

*theta = 90*t*

angle_ratio = theta/360

*S = angle_ratio*pi*DB*

base_radius = DB/2

*Xc = base_radius*cos(theta)*

*Yc = base_radius*sin(theta)*

*X = Xc+(S*sin(theta))*

*Y = Yc-(S*cos(theta))*

Z = 0

6) Using the Equatio-10 we calculate the value of β.2β is the angle between the adjacent involute curve in the gears from the centre of the base circle. Using β, we can find the position of the centre line as shown in (Figure-88).
7) Generate a plane on the position of the centre line passing through the centre of the base circle.
8) Select the involute curve and mirror this curve along the Plane generated in the previous step.
9) Project these curves and the portion of the base circle and the addendum circle between these curves and extrude cut.
10) Select this extruded cut and generate a pattern across the whole addendum circle with central axis as the centre based on the number of teeth *'N'* and the angle between them which is $\frac{360}{N}$.

For designing the ring gear, the circle that is to be extruded must be a little bigger than the addendum circle radius.

5.8 Including the gears

The way to incorporate the epi-cyclic gear train in the joints is by including the ring gear within the design itself as shown in (Figure-97). The ring gear is itself a part of the link. The planet gears will transmit motion directly to the next link. For this purpose, 3 rod type extrusions are made on the next link to hold the planet gears. The planet gears will have the freedom to rotate around these rods with the help of bearings. (Figure-96)

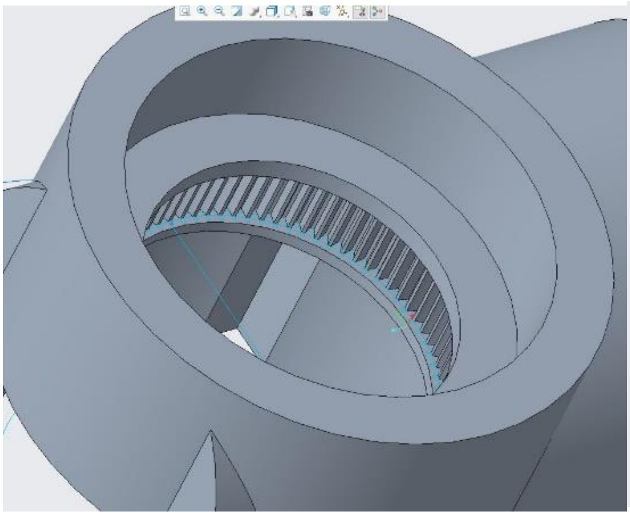

Figure 98 Ring Gear In cooperated In the Design

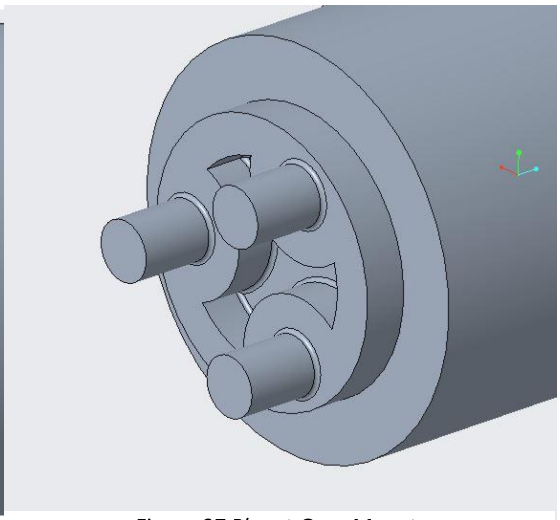

Figure 97 Planet Gear Mounts

6 Bearing

6.1 Bearing Requirements

The contact between the links during operation is inevitable. Friction must be reduced as much as possible for protection of the link material from heat, wear and tear. This will also considerably reduce the power required by the stepper motor to drive the links.

6.2 Types Of Bearing

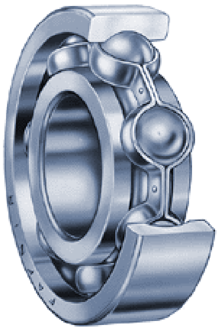

Figure 101 Ball Bearing

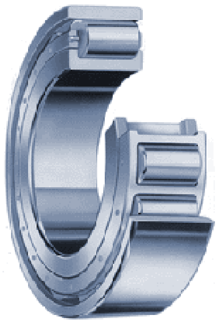

Figure 100 Roller Bearing

Figure 99 Needle Bearing

Figure 104 Ball Thrust Bearing

Figure 103 Roller Thrust Bearing

Figure 102 Tapered Roller Bearing

i. **Ball Bearings:** These type of bearings have balls within the outer and inner race. This bearing can handle both radial and thrust loads. The point of contact between each of the races and the ball is a single point. Hence the operation is very smooth but it cannot handle heavy loads as it may cause deformation of the spheres/balls and thus ruining the bearing.

ii. **Roller Bearings:** These type of bearings can handle very high radial loads. The roller between the inner and outer race is a cylinder and thus the point of contact is a line and thus it has a higher radial load carrying capacity. It is although not designed to handle thrust loads. Another variation of this type of bearing is the ***Needle Bearing*** This bearing has cylinders with very small diameters. They are specially designed for applications where not much space is available.

iii. **Ball Thrust Bearings:** This bearing is used to handle axial loads. The part that permits motion between the upper and lower race is the ball.

iv. **Roller Thrust Bearings:** These are axial load motion permitting bearings. They have a cylinder type roller to allow motion between the races and thus it has a larger axial load bearing capacity than the ball thrust bearings.

v. **Tapered Roller Bearings:** These bearings are designed to withstand large radial and thrust loads. As the name suggests, the rollers are at an angle with the race which allows the rolling movement without either of the races slipping in addition to the added load bearing capacity.

Best selection of the type of bearings for the robot

The bearings with smallest dimensions will be preferred. ***Needle Bearings*** and ***Roller Thrust Bearings*** will be used in our use case.

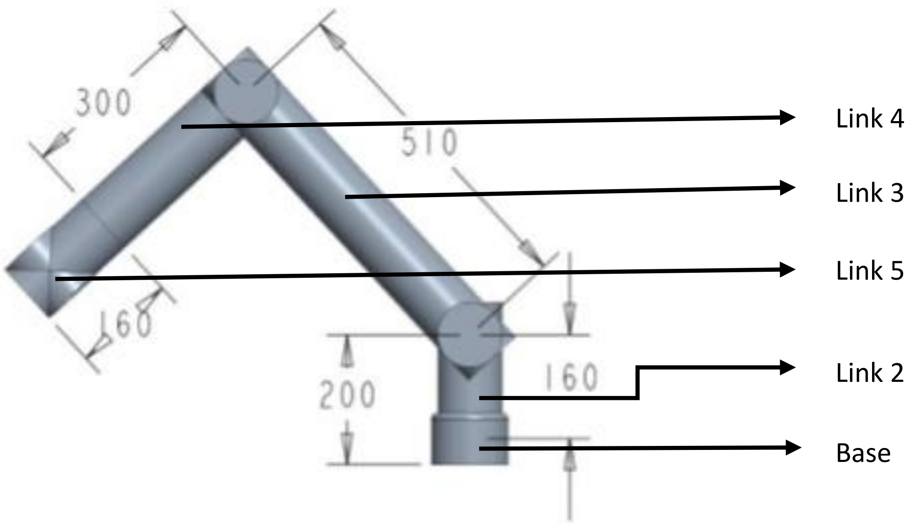

Figure 105 Assembly Dimensions

6.3 Locations of bearing placements.

For ease of troubleshooting, and uniformity, repetition of the use of bearings of same dimensions will be preferred wherever possible. Bearings of the different dimensions of the same type will only be used under absolute necessity. The design dimensions and structure will be modified based on the bearings for finalization. Refer Figure-104

a) The Base and the Link 2 will require an axial/thrust load bearing capacity to allow the rotation of link 2 over the base. Only one such bearing is required. ***Roller Thrust Bearings*** will be used at this location.
b) The Base and Link 2 will also require ***Needle Bearings*** for the external side contact. One bearing is required for this purpose.

c) Wherever there is contact between different links, the bearings are required as there is relative motion required between each of the connected links. They are the joint locations. They are required between Link 2-Link 3 and Link 3-Link 4. There will be a requirement of 2 ***Needle Bearings*** of the same dimensions.

d) Requirement of using bearings between the 3 extruded rods and the planetary gears that will be fixed on them as shown in Figure-96. The mechanism discussed in **Section 5.8** will be used in the linkage between Link 2-Base, Link 2-Link 3, Link 3-Link 4. Each linkage will require 3 bearings based on Figure-96. There is a total of 3 linkages with each requiring 3 bearings. Hence the total will be 3x3 = 9 ***Needle Bearings*** of the same dimension.

For later use and easier recall let us name each of the different bearings mentioned in *'a', 'b', 'c' and 'd' as* ***'A', 'B','C'*** *and* ***'D'*** *respectively.*

6.4 Bearing Specifications:

We require 4 types of bearings. The best fit from the standard bearing specifications are mentioned in Table-8

Table 8 Specifications and Number Of Bearing Used

Bearing	***Bearing Type***	***Count***	***Internal Diameter (mm)***	***Outer Diameter (mm)***	***Width (mm)***
A	Roller Thrust	1	70	95	6
B	Needle	1	100	120	25
C	Needle	2	70	95	25
D	Needle	9	15	27	16

7 *Finalizing the design of the robot*

Changes have to be made in the earlier design to include the bearings and also for holding the motors. The main dimension deciding criteria will be the dimensions of the bearing and also the size of the stepper motors required.

The final design stage will include:

- ❖ Design and assembly along with well-defined joints
- ❖ Motion analysis of the assembly along with motion contact of gears
- ❖ Stress analysis for removing any unnecessary weight from the design
- ❖ Finalizing design based on above results

7.1 **Motion Analysis**

Motion analysis was successfully tested using Inspire by defining all the criteria required for analysis. (Refer Section 3.1 for steps). The motion was strictly obtained through stepper motors whose torque was multiplied by motion contact from gears.

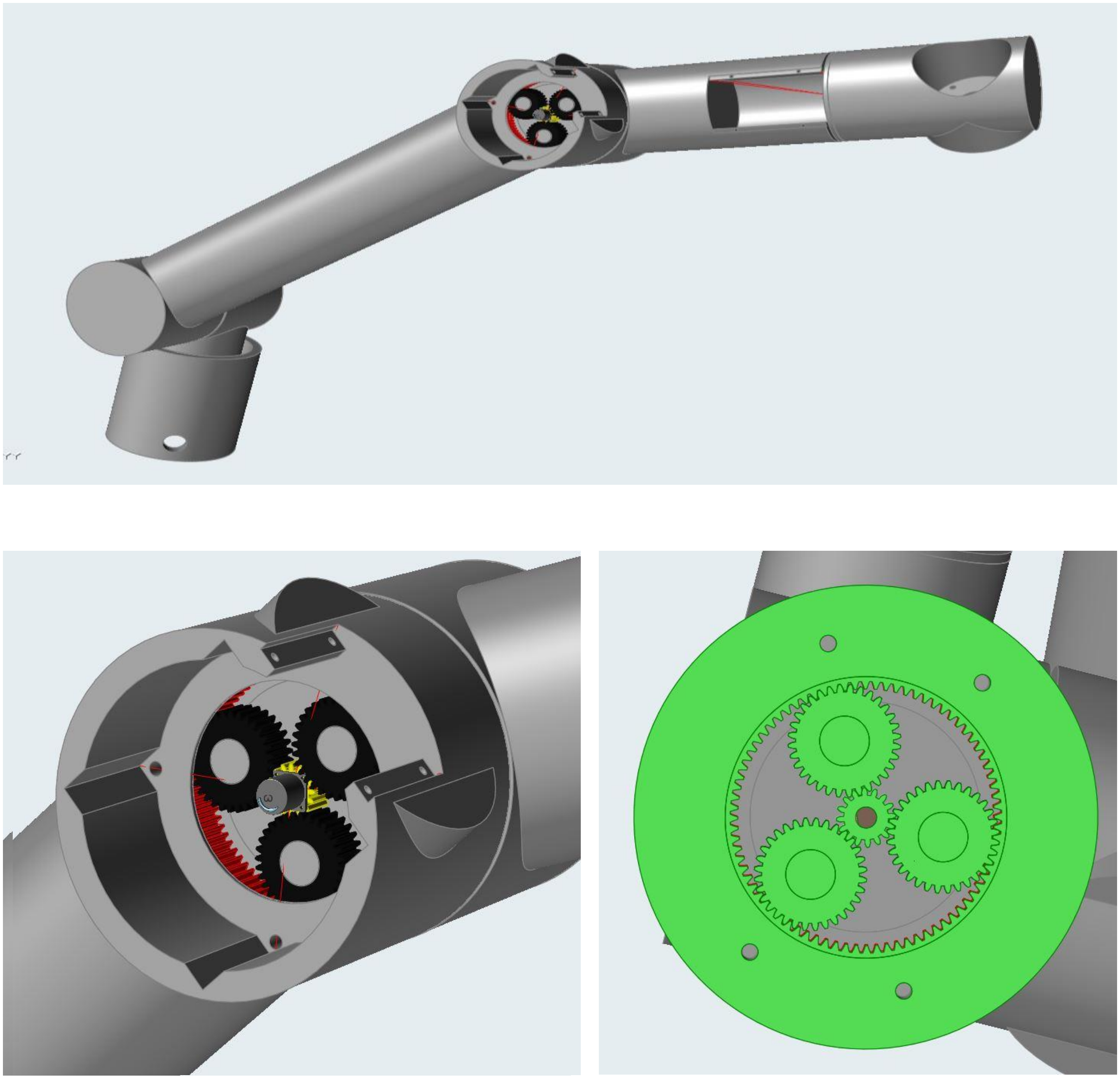

Figure 106 Motion Analysis on Inspire

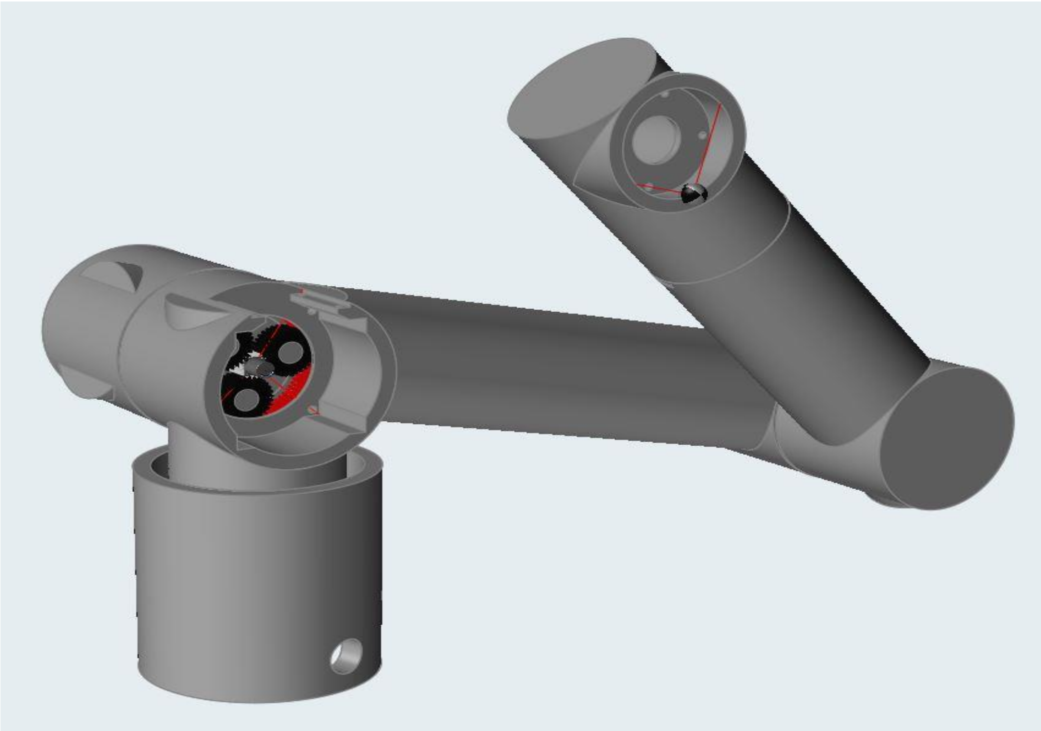

Figure 107 Motion Analysis on Inspire

7.2 **Stress Analysis**

Stress analysis and topological optimization of the links were done to reduce the weight of the assembly as a whole. Topological optimization refers to the removal of material from the region of the part where the mass does not add up to the structural strength of the part. One of the motives of the designing the manipulator is to make is as light as possible for handling and cost cutting purpose. The stress analysis and topological optimization simultaneously can be done using Altire Inspire software. The steps and the procedure to perform stress analysis and topological optimization using Altire Inspire are mentioned below: -

1. Import the design file of the part whose optimization is to be done to the software.
2. Select geometry tools from the top bas as shown in the Figure-105

Figure 108 Geometry Tools in Tool Category Bar

3. To obtain better and fast results the design has to be simplified for removing tapers, roundness, holes, etc. To simply the design the simplify tool is used from the geometry tools. This tool contains various types of simplifications, namely Imprints, rounds, holes and plugs and is advanced enough to find out the parts by itself where this operation can be done. Just by clicking on the found parts the operator can simplify the design where ever required.

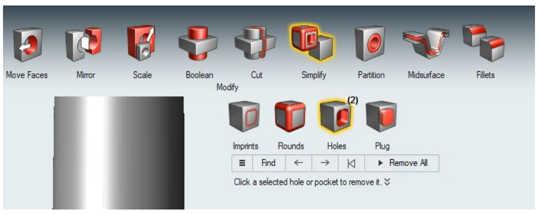

Figure 109 Simplify Tool

4. After simplifying the design, cut tool in the geometry tools is used to divide the design into different parts to ease defining Design Space (Design Space refers to the region of interest where the operation of topological optimizations has to be performed).

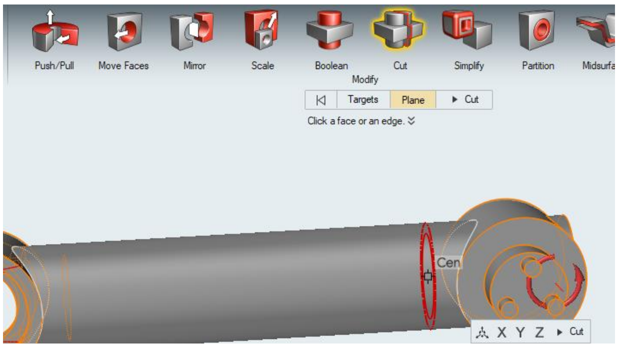

Figure 110 Cut Tool

5. Now it is time to define the design space. From the cut parts select one part which has to be included in the design space and right click on it to get the options. Then tick the

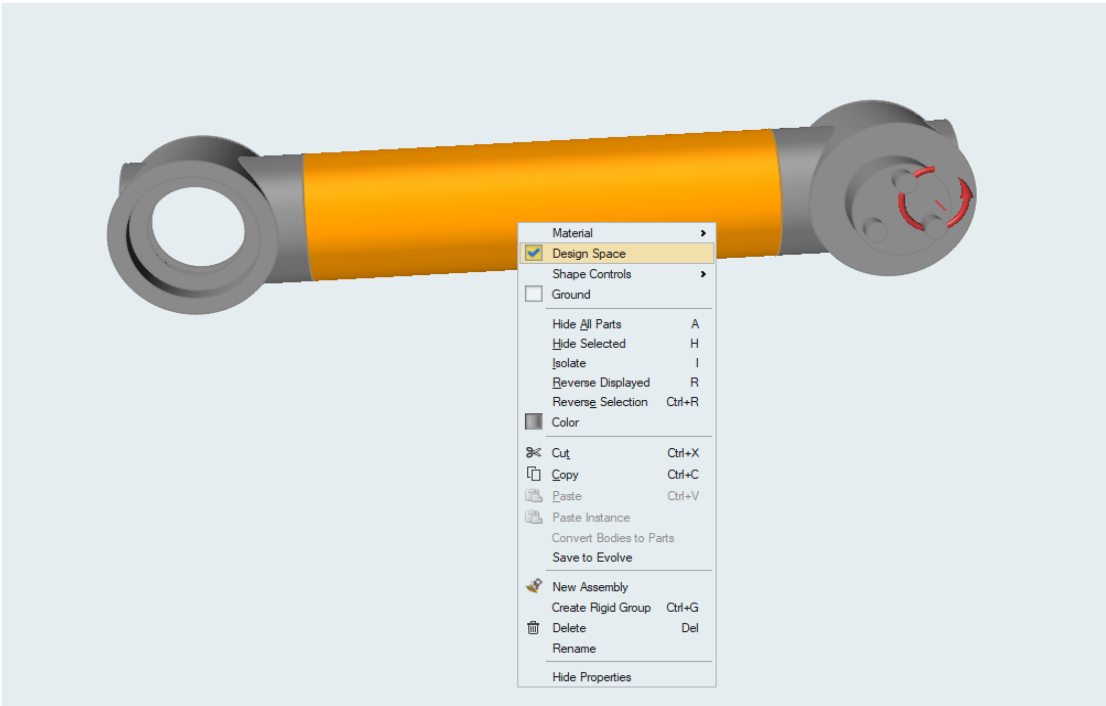

Figure 111 Defining Design Space

box which say design space. Do the same for all other parts which are to be included in the design space.

6. The next step to perform the topological optimization is to apply constraints. From the bar select the structure tools as shown in the Figure-109

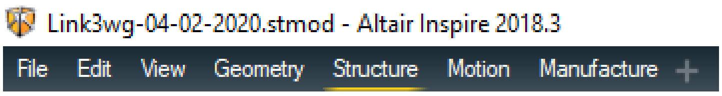

Figure 112 Structure Tools In Tool Category Bar

7. Select Loads tool from the structure tools. This tool helps applying numerous loads (namely point load, torsional load and surface load) and also different supports by selecting different points on the load icon itself. Apply loads and define their positions as per the requirement using this tool and editing the parameters as shown in the Figure-110

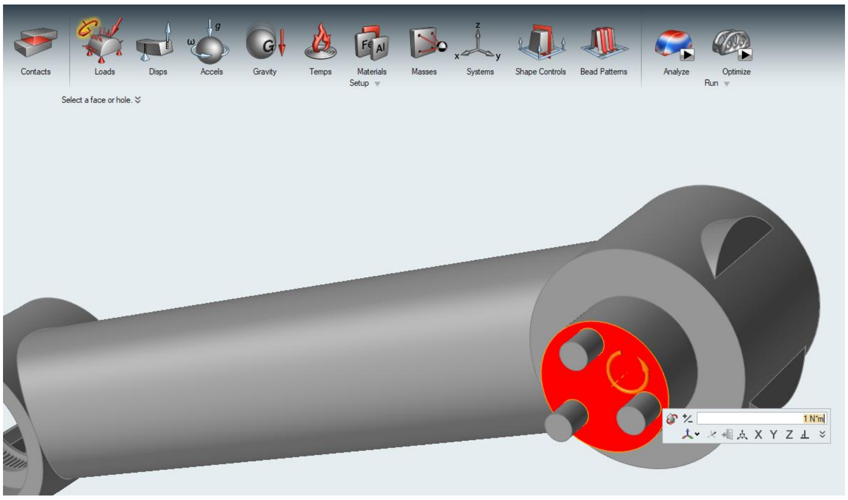

Figure 113 Load Defining Tool

8. Now select optimize tool from the structure tools by clicking on the play button of the optimize icon as shown in the Figure-111

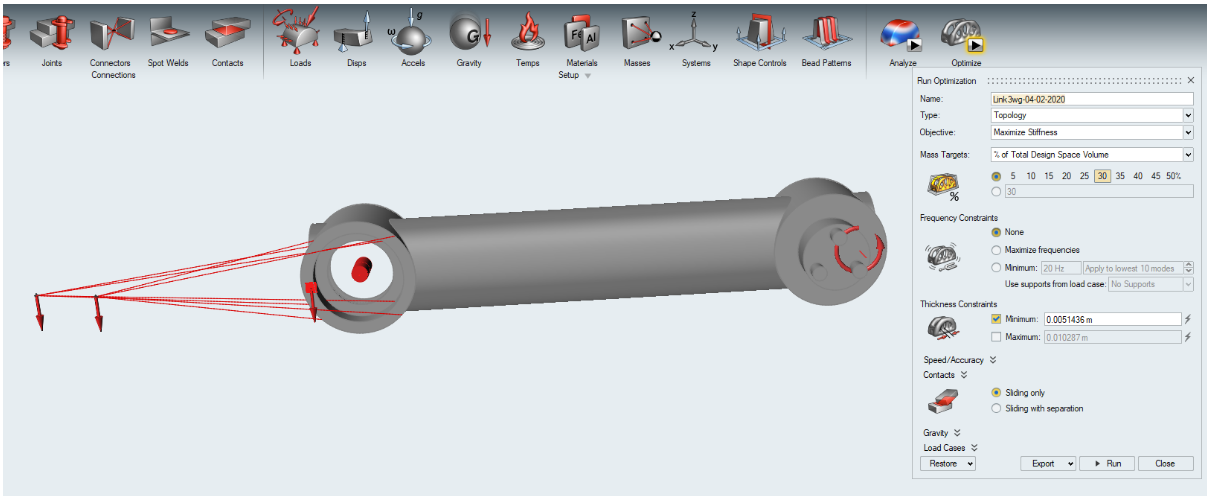

Figure 114 Optimize Tool

9. The parameters for optimization available that can be changed according to the requirement are as shown in the Figure-112
    - **Type:** Includes the type of optimization to be done. It contains mainly 4 optimizing modes (topology, topography, gauge and lattice). In this case we are using topological optimization.
    - **Objective:** It refers to the main focus of the optimization. Objectives are mainly of 3 types (maximize stiffness, maximize frequency & minimize mass). From this we are working on maximizing the stiffness.
    - **Mass Target:** It refers to the minimum percentage of mass to be kept untouched and rest can be removed. (this figure can be played around with to get required results)
    - **Frequency constraints:** These are used where the resonance also plays a role in the application of the designed part. in this case there is no need for the frequency constraint because there are no external vibrations involved in the application of manipulator.

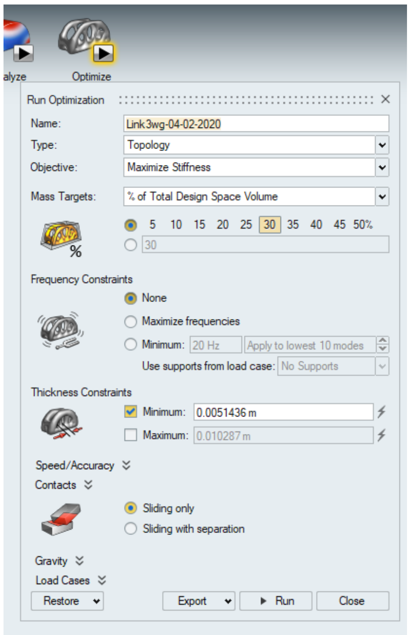

Figure 115 Parameters For Optimization

    - **Thickness constraints:** As this software creates mesh automatically according to the design, the mesh size can be controlled by this parameter to choose the accuracy, details and precession of the result obtained. By decreasing the mesh size the accuracy, precession and details of the result are increased but the time for calculation also increased drastically.
    - **Contact:** It refers to the selection of the fatigue and failure type for the optimization whether the failure is allowed to separate parts or not. Here we are using sliding only.
    - **Gravity:** It gives the freedom to the operator to include gravity also as a factor for calculation or not. Here we have defined the gravity of the design at the required direction and have included the gravity factor for calculation (because the design has a significant weight and hence the gravity will play a significant role).

    Set the parameters from the options available as per the requirement and click on Run.

10. The Run Status window will pop up onto the screen and the optimization calculations have begun. Wait for it to get completed (it may take up to several hours and even days

depending upon the processor of the device and the amount or complexity of calculations involved)

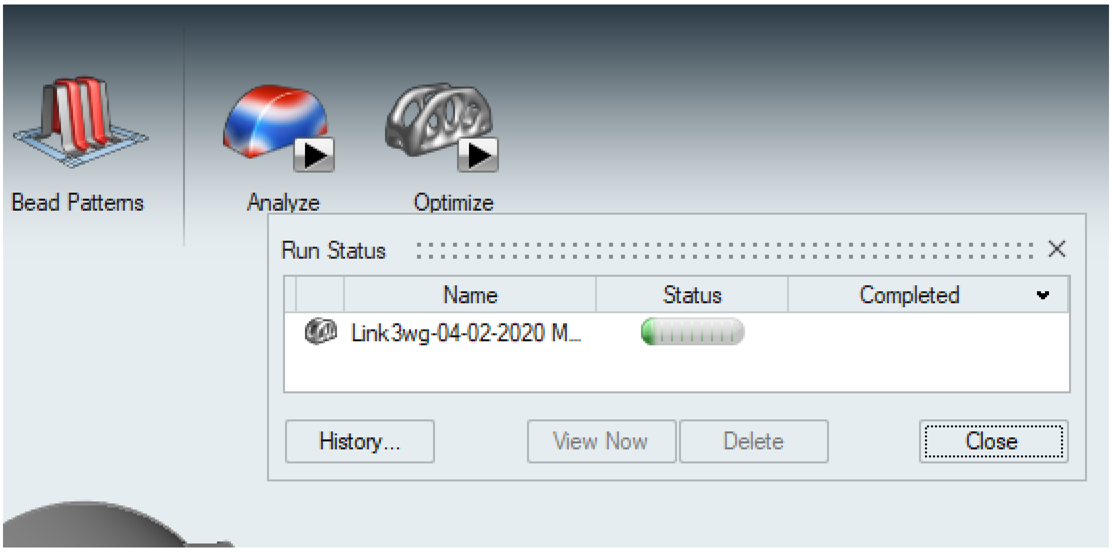

Figure 116 Run Status Window

11. After the completion of the process the tick will appear on the Run Status. Double click on the file to open the result as shown in the Figure-114

Figure 117 Topologically Optimized Part

The final design layout of each individual part is shown in figures below:

The next step in the process is to 3D print the final design. There are various factors that decide the quality and time required to print.

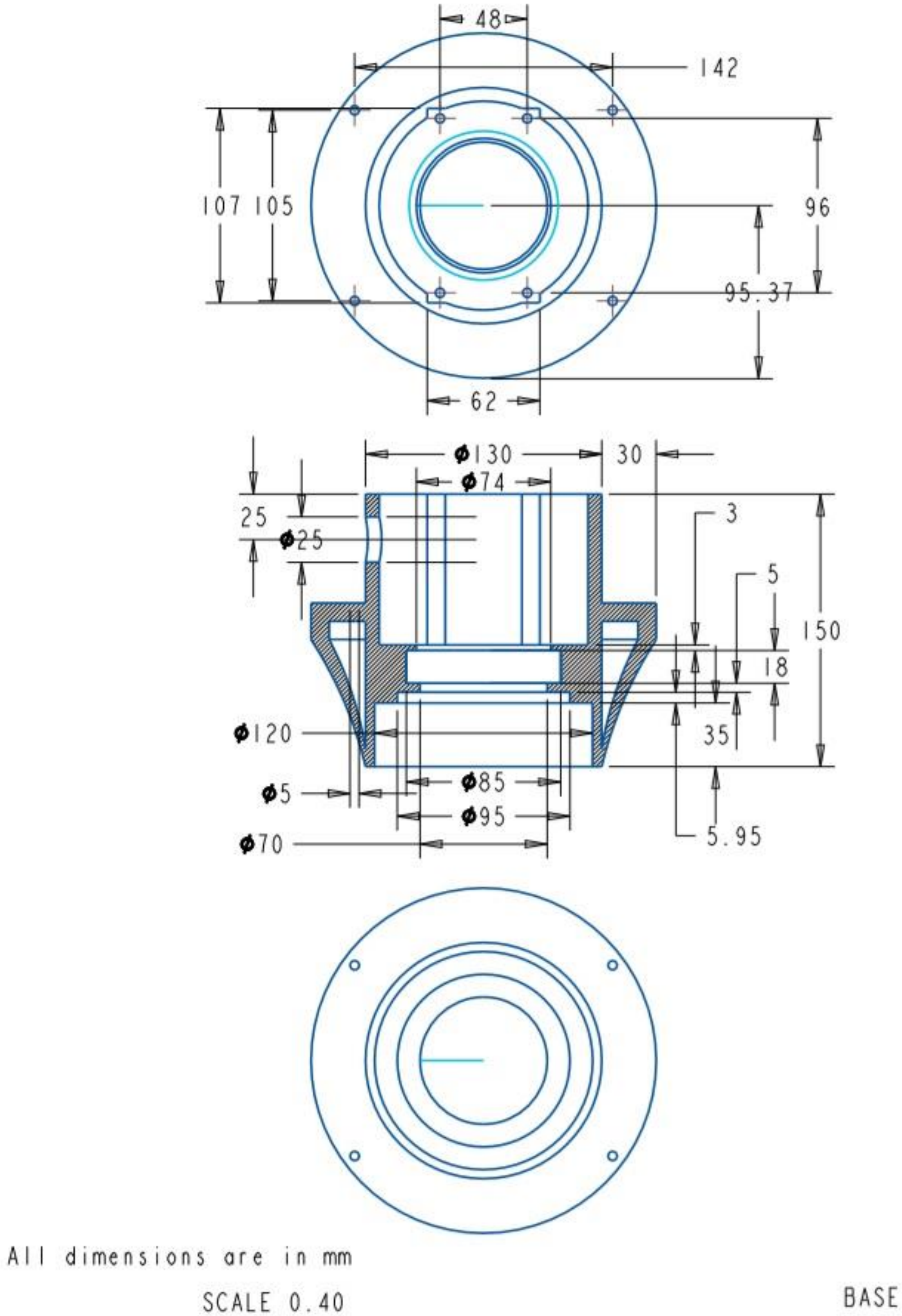

Figure 118 Base CAD Drawing

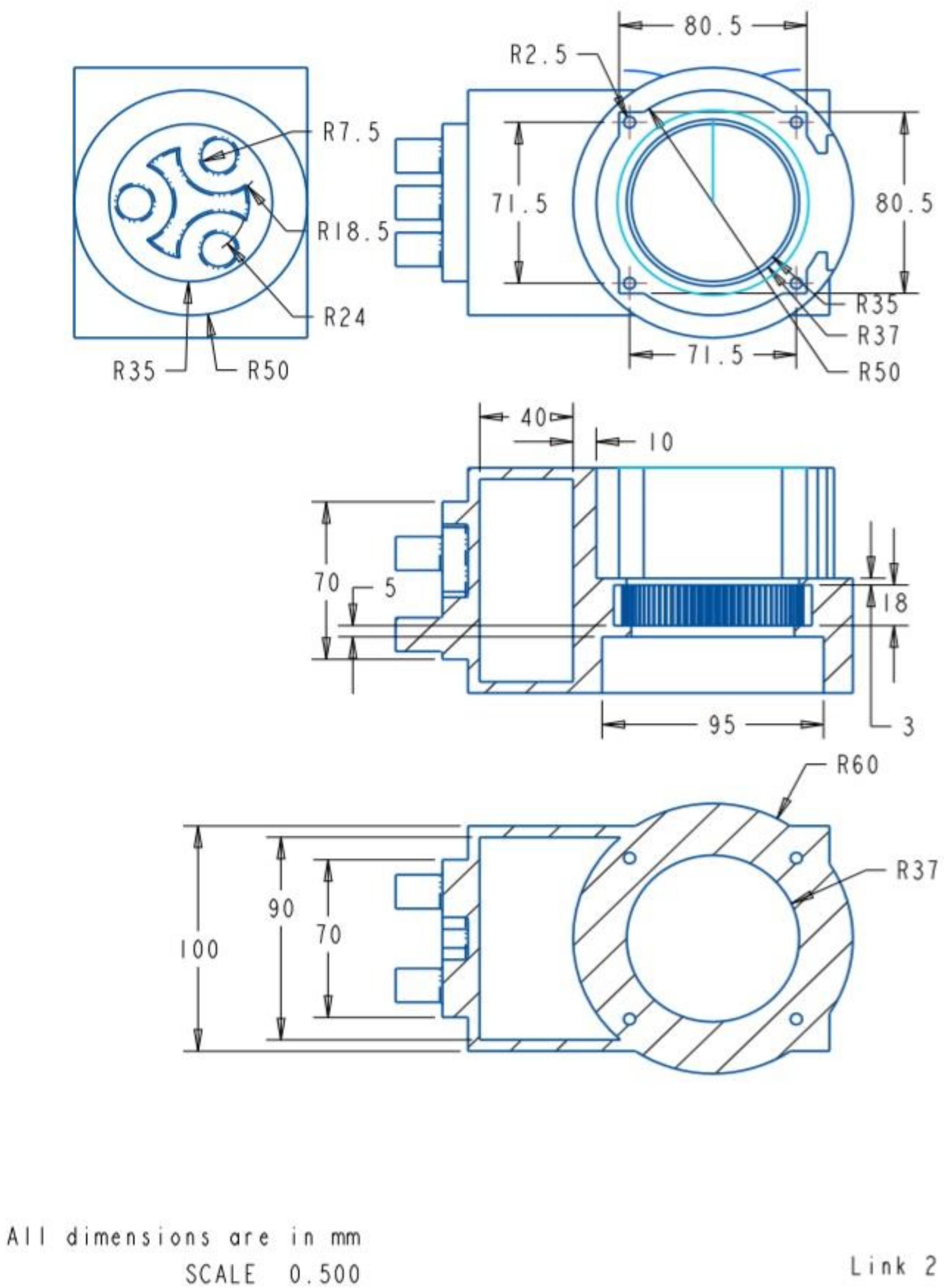

Figure 119 Link 2 CAD Drawing

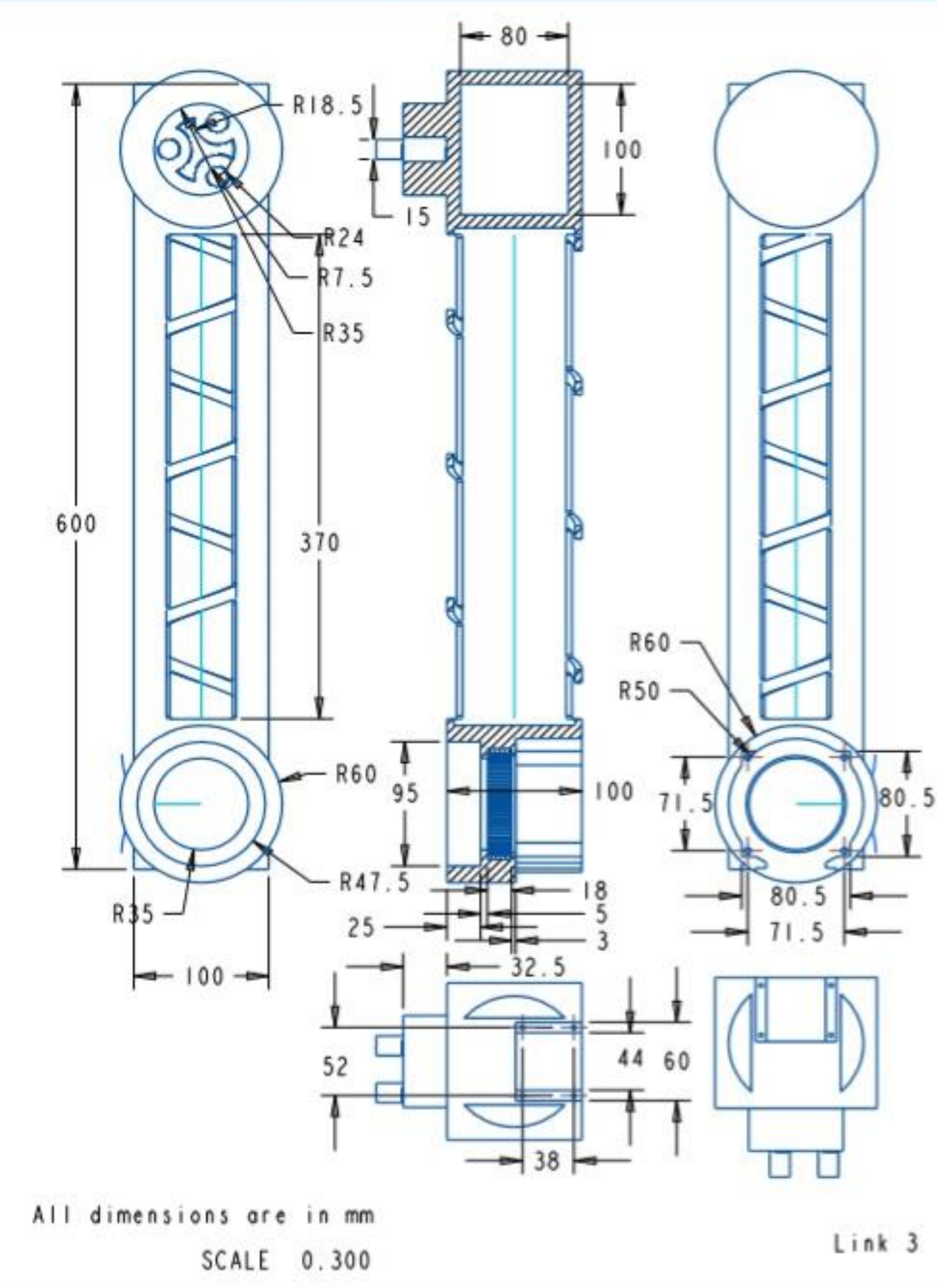

Figure 120 Link 3 CAD Drawing

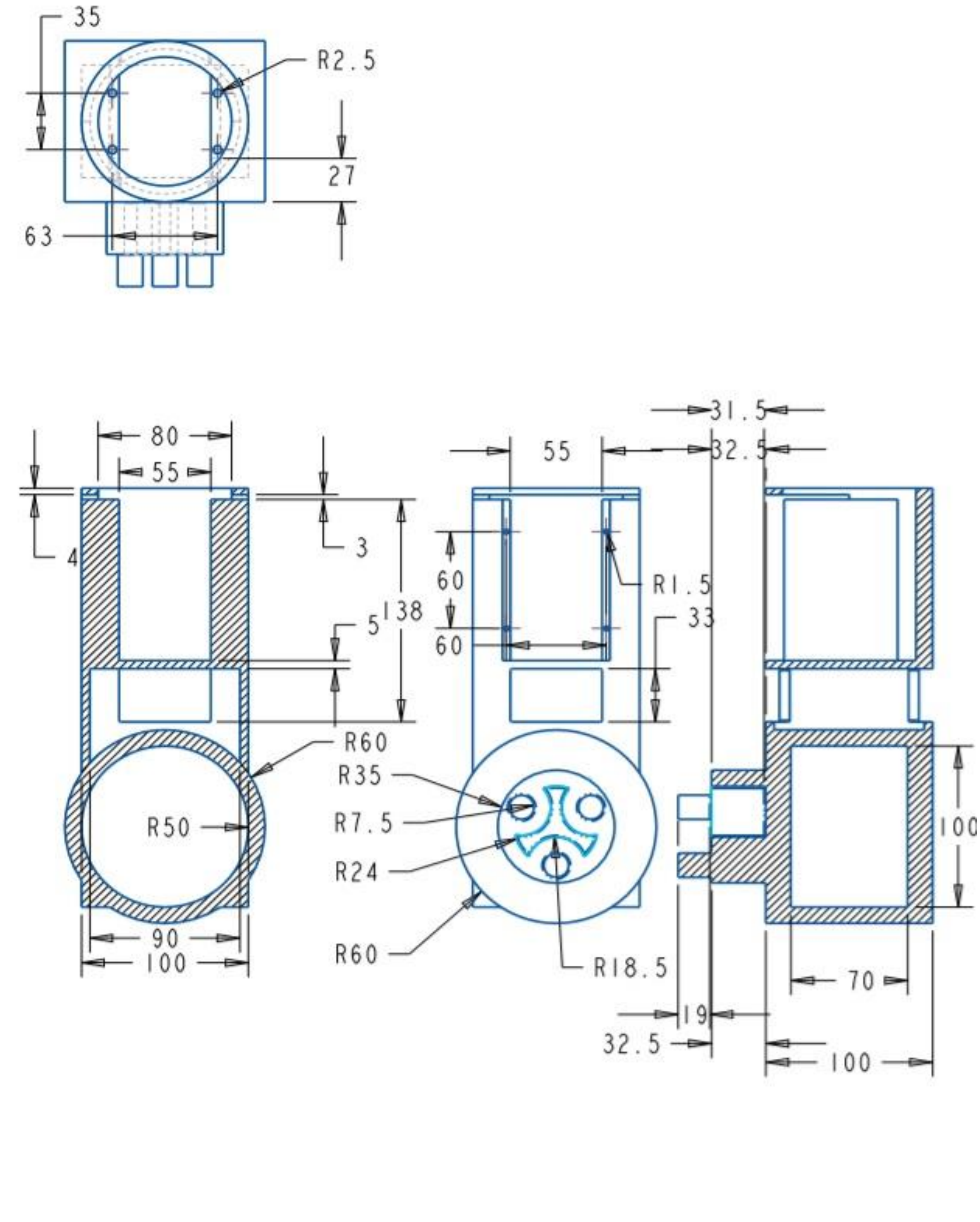

Figure 121 Link 4 CAD Drawing

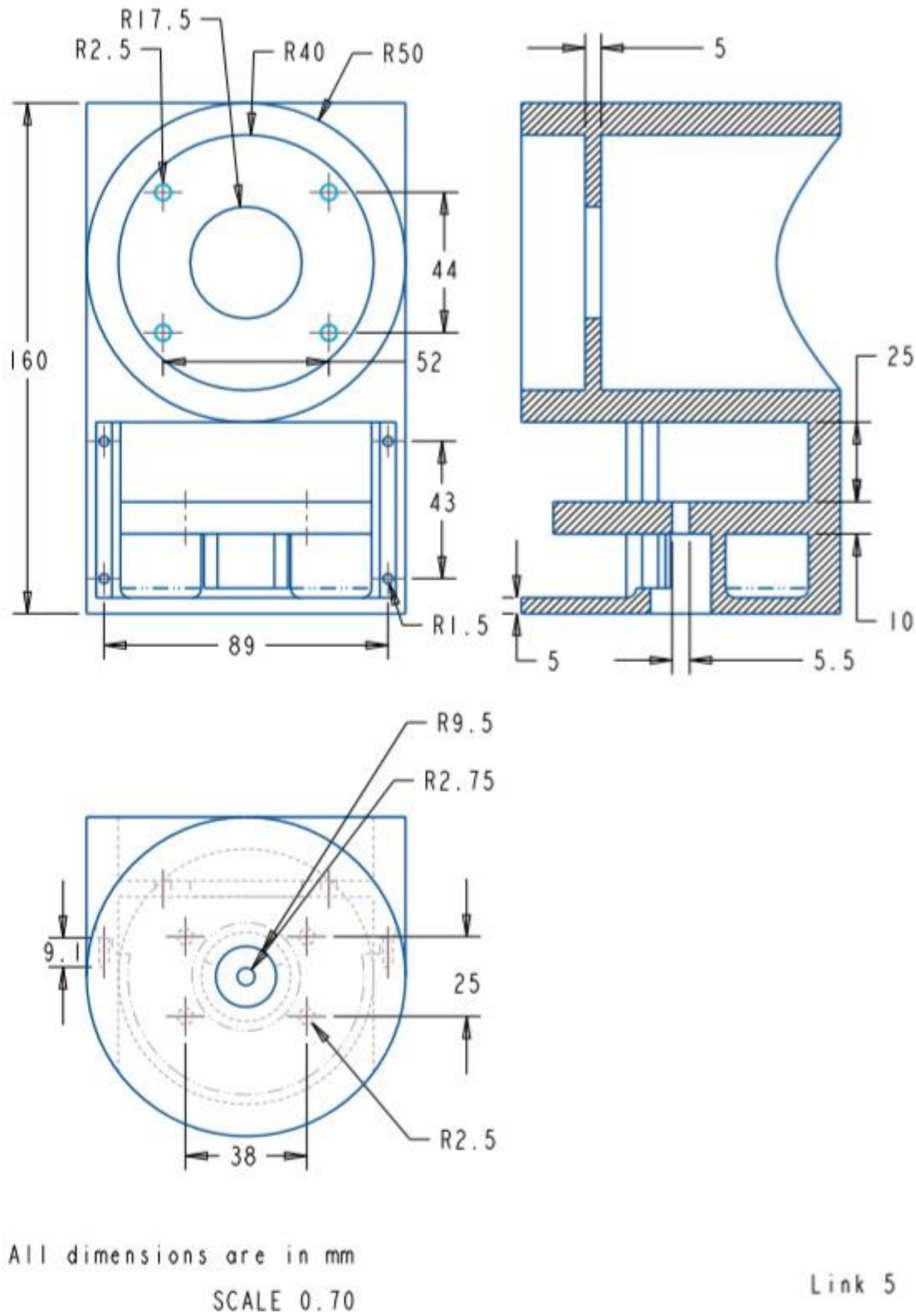

Figure 122 Link 5 CAD Drawing

8 3D Printing: -

3D printing is the technique used for rapid prototyping complex designs. The material used for 3D printing was selected to be ABS because of its high tensile, torsional strength and higher melting point when compared to its competitors. The orientation of the printing is also kept in consideration to gain higher strength at required regions. Orientation of the print not only determines the strength of the part printed but also helps reducing the material used for supports and the reducing the time taken for the operation. the parameters are changed and the results are visualized and analyzed using 3D printing software (in this case we used Ultimaker CURA 4.4). Using 3D printing techniques, the following parameters can be altered and tested visually at the software to get best results as per the requirements: -

1. **Orientation**
   The orientation refers to the geometric configuration of the part with respect to printer using visual slicing software. The geometric configuration is the layout and position the part is made to be printed in the 3D printer. This determined the torsional, bending as well as the tension strength of the part.

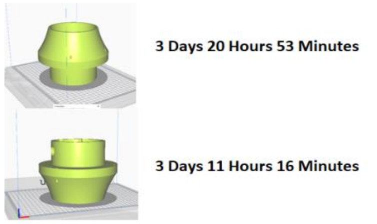

Figure 123 Orientation effect on Time of Print

2. **Nozzle size**
   The nozzle size determines the amount of material coming out of the nozzle. Nozzle size therefore determines thickness of the layer. Greater the layer thickness, less detailed features can be printed, weaker is the contact between the layers leading to weak strength but less is the time taken for printing. By using a great combination of this parameter we can achieve the best printed product with practically decided strength required.

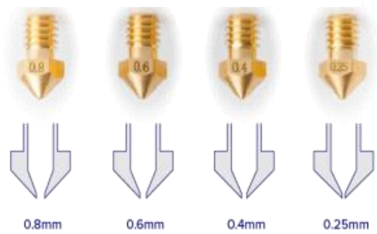

Figure 124 Nozzle Size

3. **Infill percentage**
   Infill is another parameter which plays an important role in the printing process. Infill determines the weight, strength and the time taken for the printing process. Greater the infill percentage the stronger is the strength, more is the time taken for the printing process and more is the weight.

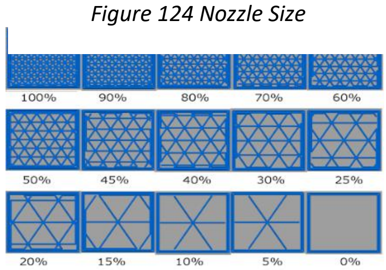

Figure 125 Infill Percentage

4. **Infill type**
   Infill type also has a significant but less role in determining the strength of the part printed. Among all triangular has the most strength and also has an insignificant increase in the time taken to print.

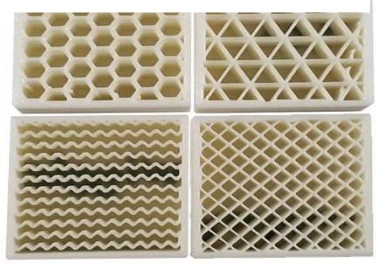

Figure 126 Infill Type

Every part of the assembly is individually assessed and the best parameters for each part are set for the best possible combination.

Table 9 Base 3D Printing parameters

	Type of Infill	Amount of material		Print Time
		Structure	**Support**	
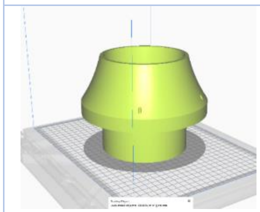	triangular	829	290	3days 20 hours 53 minutes
	cross 3d	680	290	3days 16 hours 19minutes
	zig zag	824	290	3days 20hours 50 minutes
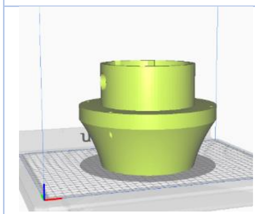	triangular	828	120	3days 11hours 16minutes
	zig zag	824	120	3days 10hours 47minutes
	gyroid	816	120	3days 16hours 10minutes

Table 10 Link-2 3D Printing parameters

	Type of Infill	Amount of material used (gm)		Print Time
		Structure	**Support**	
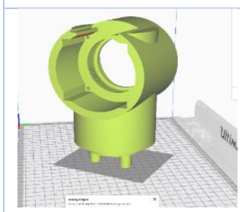	triangular	507	161	2days 8hours 2 minutes
	zig zag	504	161	2days 7hours 50minutes
	gyroid	499	161	2days 11 hours 4minutes
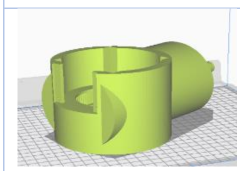	triangular	506	61	2days 1hour 42minutes
	zig zag	504	61	2days 1hour 42minutes
	gyroid	499	61	2days 4hours 52minutes
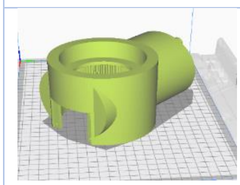	triangular	506	93	2days 3hours 49minutes
	zig zag	504	93	2days 3hours 43minutes
	gyroid	500	93	2days 7hours 1minute

Table 11 Link-5 3D Printing parameters

	Type of Infill	Amount of material used (gm)		Print Time
		Structure	Support	
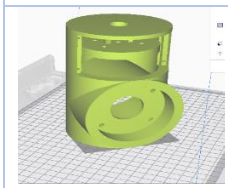	triangular	469	117	1day 23hour 34minutes
	zig zag	467	117	1day 23hour 29 minutes
	gyroid	462	117	2days 2hours 40minutes
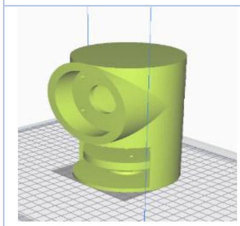	triangular	469	119	2days 0hours 10minutes
	zig zag	468	119	2days 0hours 6minutes
	gyroid	462	119	2days 3hours 10minutes
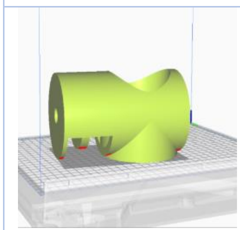	triangular	468	58	1day 19hours 31minutes
	zig zag	468	58	1day 19hours 25minutes
	gyroid	458	58	1day 22hours 29minutes

Table 12 Link-3 3D Printing parameters

	Type of Infill	Amount of material used (gm)		Print Time
		Structure	Support	
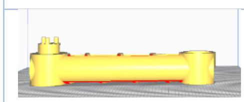	triangular	1529	0	3day 20hours 56minutes

Table 13 Link-4 3D Printing parameters

	Type of Infill	Amount of material used (gm)		Print Time
		Structure	Support	
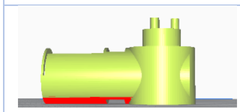	triangular	1053	0	2days 12hours 00minutes

Figure 127 3D Printed links and gears

9 ACTUATION SYSYTEM

9.1 Introduction:

The robot has 4 degrees of freedom as proved in *Equation 3 Grubler's formula.* There are 5 main links in the robot out of which 4 are movable. The *Base* is fixed. The rest of the parts are to be given motion. There are various types of motors used in robotics. Some of the most popular types are:

AC motors:

The Alternating Current motors are widely used in many applications. In robotics however many components rely on DC electronic parts and hence for synchronicity these kinds of motors are rarely used.

DC Motors:

They run on Direct Current. These motors have a high torque to inertia ratio and are capable of running at very high speeds. Controlling speeds and changing directions is quite easy. There are mainly two types of DC motors namely *Brushed DC motors* and *Brushless DC motors*.

- Brushed DC motors: These motors are the found in toys, cooling fans, etc. The magnetic field is used to drive a set of electrical coils which are attached to a ring known as a commutator. This commutator gets electricity from two metallic brushes that make contact with different segments of the coil at a particular instant. Hence a lot of heat is generated due to friction.
- Brushless DC motors: These motors use permanent magnets as a rotor and numerous coils as a stator. The Lorentz force drives the motor this way without any contact and hence without any friction and heat loss. They require electrical commutation instead of mechanical. In order to determine the position of the shaft, sensors are crucial. The control of the currents requires controllers.

Comparing *Brushless DC motor* and *Brushed DC motor*, it is clear that the Brushless DC motor lasts relatively longer. Brushless DC motors have very high power density, extremely high dynamic response. The range of speed the BLDC offers is much higher along with higher efficiency when compared to Brushed DC motors. But the complexity and intricacy of the design makes the cost of Brushless DC motor relatively high. Repairing these motors may not prove to be as effective. The Brushed DC motors have relatively lower speed ranges to offer, lower power efficiency due to the fact that a lot of heat is generated in this design due to constant friction. But this allows for a relatively simple design, extremely easy to repair and can be replaced effectively as manufacturers provide the life of the brushes. The difference in the prices of the Brushless DC motors and the Brushed DC motors is astronomical. Brushed DC motors are very cheap. The installation of the brushed design is easier. The Brushless DC motors require electrical controllers which also add to the costs.

Stepper Motors:

These are also a type of DC motor. But they are close to the highly efficient brushless design. It consists of a permanent magnet as the rotor cut in gear shape which is surrounded by evenly spaced wire windings which attract or repel the permanent magnet and thus causing the rotation. Because of this design, it is able to move in precise steps. This design has many advantages and disadvantages at the same time.

Comparing DC motors and Stepper Motors:

The common Brushed DC motors are easier to control when compared to stepper motors. They only require input voltage at its two leads to make it operational. Speed, directional control is all done by regulating the voltage. But stepper motors require some form of microcontroller to control the current in the stator windings. Stepper motors are not meant for continuous use, they are designed specifically to move in discreet steps. DC motors provide higher rpm. The range of stepper motors typically is within 2000 rpm. Modern DC motors are designed for very high power efficiency reaching up to 85%. The stepper motors on the other hand consume current at maximum load. Thus we can conclude that the power efficiency of DC motors is relatively higher than stepper motors. Due to this reason stepper motors can provide maximum torque at lower speeds as well while the DC motors cannot. This allows for positive torque values at 0 rpm in stepper motors. They are more accurate and precise in their angular movement and hence, stepper motors are preferred in applications like CNC, 3D printing and robotics where high precision is required. As for the cost, both the brushed DC motors and Stepper motors are inexpensive.

Why stepper motors?

Both the brushed DC motors and stepper motors are inexpensive so cost is not a major deciding factor. In industrial robots use case, higher accuracy, reliability and torque holding capacity is preferred over higher efficiency and ease of control. While both have high torque capacity, only stepper motors push it to the maximum even at low speeds which will prove to be beneficial. Therefore for actuation purposes, Stepper motors are selected. [7]

9.2 Working of stepper motor

Stepper motor is a DC motor that rotates in steps. Stepper motor works on the principle of rotating a centralised permanent magnet by creating an electromagnetic field around it by energizing different coils at different times. One or more coils also be energized at a time according to the type of step required.

Steps of a stepper motor can be explained by the assembly shown below

When at a time only one coil is energized to move the permanent magnet placed at the centre in an order to rotate the magnet unidirectional, the motor is said to be wave drive as shown in the Figure-

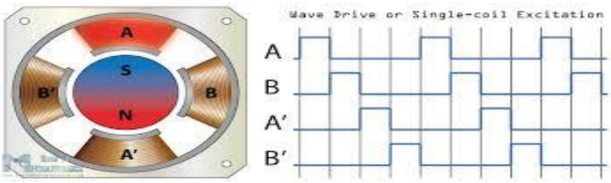

Figure 128 Wave drive

When the alternate coils are activated simultaneously to rotate the centre magnet to get a greater torque than by activating single coil at a time is called full step drive. As shown in the Figure-

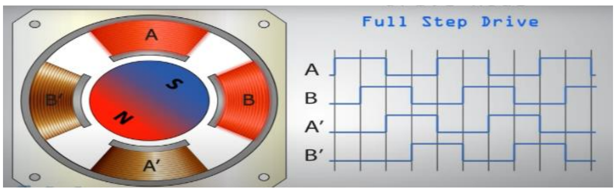

Figure 129 Full Step drive

The specifications of Wave drive and Full step drive motors are combined together to form half step drive motor with one coil and then two adjacent coils are energized and then this cycle repeats as shown in the Figure-

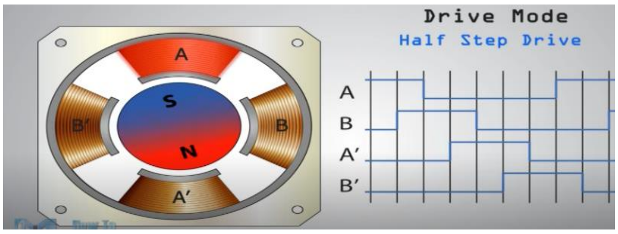

Figure 130 Half Step drive

To reduce the step size for more accuracy the number of coils can be increased.

Stepper motors can be divided on the basis of various assembly as shown below: -

1. Permanent Magnet Stepper Motor : it consists of a permanent magnet in the centre and surrounded by coils which when energized in act as an electromagnet. The coils are energized in different patterns to rotate the centre magnet to a specific angle.
2. Variable Reluctant Stepper Motor : in this type of stepper motor, the permanent magnet is replaced with a "cross" shaped conductor which aligns to the position every time where there is the least gap between the conductor end. The coils are energized in a specific order according to the step size and the direction of movement of the output (that is the conductor at the centre).
3. Hybrid Synchronous Stepper Motor: It is the motor combined specification of both permanent and variable reluctant type of stepper motor. Its assembly includes a permanent magnet shaped in the form of a sprocket surrounded by coils shaped according to the permanent magnet shape as shown in the Figure-

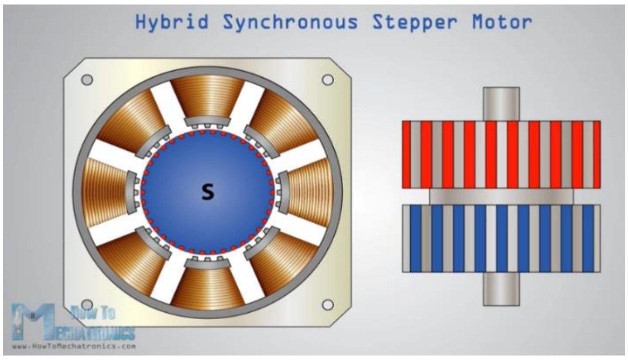

Figure 131 Hybrid Synchronous motor

Hybrid Synchronous stepper motor is most convenient type of stepper motor to be used for robotic manipulator due to its high accuracy and high holding torque.[8]

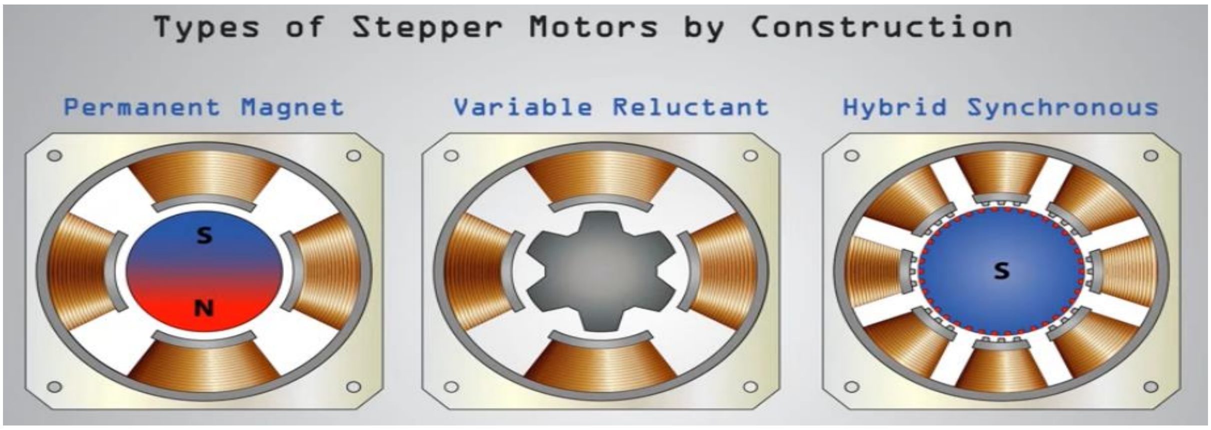

Figure 132 Different types of stepper motor

9.3 Motor Selection

Based on the motion analysis of the design we can estimate the torque capacity required for the motors to control the links. The approximate torque capacity of the required motors are listed in the table below:

Table 14 Selected Stepper Motors

Motor Type	Holding Torque	Count
Nema 23	1.8 Nm	2
Nema 23	1 Nm	1
Nema 17	0.45 Nm	1

9.4 Controller programming unit

There are majorly two types of controlling units that can be put into consideration, ie. Arduino Uno and Raspberry Pi. The comparission of arduino uno and raspberry pi can be done on the following basis.

1. Type of circuit: the Raspberry Pi is a mini-computer whereas Arduino Uno is a micro-controler therefore arduino uno is less capable of performing complex operations.
2. Speed of processing: Raspberry pi has a computing speed 40 times than that of the Arduino uno. Therefore operation can be performed faster on the raspberry pi than that on Arduino uno.
3. Operating system: Arduino uno has no operating system of its own, it only interprets the codes written to it whereas Raspberry pi has its own operating system called Raspbian. It consists all features of a computer namely processor, graphic driver and memory. Raspbian has a user interface similar to windows and is operated using mouse, keyboard and a display screen.
4. Performance capability: where Arduino uno is only capable of performing repeatitive tasks like switching on and off lights, opening and shutting of gate, creating theft alarm and mail if any tresspasser, on the other Raspberry pi can be used for multiple complex tasks like atomated driving or operations using computer vision are to performed.
5. Coding Language: Raspberry Pi uses global coding languages like C++, C and Python whereas Arduino Uno uses its own coding language named Arduino which is way similar to C language.

To program a robotic manipulator it involves a complex set of calculation, machine learing and computer vision which make Raspberry Pi more reasonable to be used.

Figure 134 Raspberry Pi

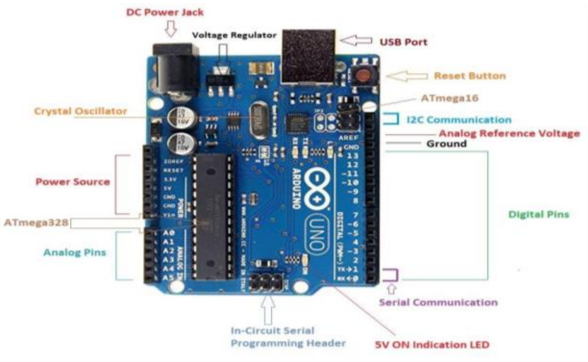

Figure 133 Arduino Uno

9.5 Motor Driver (DRV-8825)

Motor Driver: Motor driver acts as an amplifier to convert low current signal received from the controlling unit into high current signal and fed to the motor. It basically acts as an interface between the control unit and the motor itself. A control unit usually operates on low current and voltage. Motors require high current values which cannot be directly provided and directed by the controller. Motor driver includes ports to be connected to both each offering various functionality as designed by the driver manufacturer which can finally be used for communication between the motor driver, controller and the motor. Motor driver can be used as an intermediate to externally powering the motor using a battery as higher current values can break the controller unit. There are various types of motor driver are available in the market, they are differentiated by the component code written and the functionality it provides on the driver itself. The type of controlling unit (Arduino Uno, Raspberry Pi, etc.) used and the type of motor (Stepper motor, Servomotor, etc.) used determines which motor driver has to be used.**[9]**

The motor driver suitable for the use of a robotic manipulator using raspberry pi 3 is DRV-8825. It has the following features: -

- Can drive a motor with 2.2 amp and 45 volts
- Adjustable current chopper driver
- Thermal and electrical protection
- 6 step resolutions (from 4 steps to 132 steps)
- Built in 3.3V regulator make it pi friendly

The various ports of the motor driver are explained below: -

1. GND pin: it is connected to the ground pin of the raspberry pi
2. STEP pin: the step pin is connected to the GPIO 21 pin of the raspberry pi. This is to move the motor in steps.
3. DIR pin: the direction pin is connected to the GPIO 20 pin of the raspberry pi. This pin is set programmatically to control the direction of the movement of the motor.
4. SLP and RST pins: the sleep and reset pins are the default low of the motor driver and are connected to the 3.3 voltage supply of the raspberry pi. This voltage is used as a holding torque of the stepper motor.
5. VMOT pin: it is connected to the positive terminal of the external supply.
6. GND pin: it is connected to the negative terminal of the external supply.
7. Vref potentiometer: it is used to set the maximum motor current. According to the data sheet the maximum current is 1A for the motor driver DRV-8825 and the relation between the Vref and the current is given by
   $$Current = Vref\ X\ 2$$
   Therefore the Vref for the maximum current is 0.5 V from the above equation.
8. Vref Via: this is used to measure the voltage controlled by the Vref potentiometer. The Vref should not be set higher than 0.5 V according to the calculation done for the motor driver DRV-8825
9. B1, B2, A1, A2 pins: these pins are connected to the motor pins. These pins give power to the motor to rotate.
10. M0, M1, M2 pins: these pins are used to programmatically to be set anywhere from full set to 32 micro-steps.

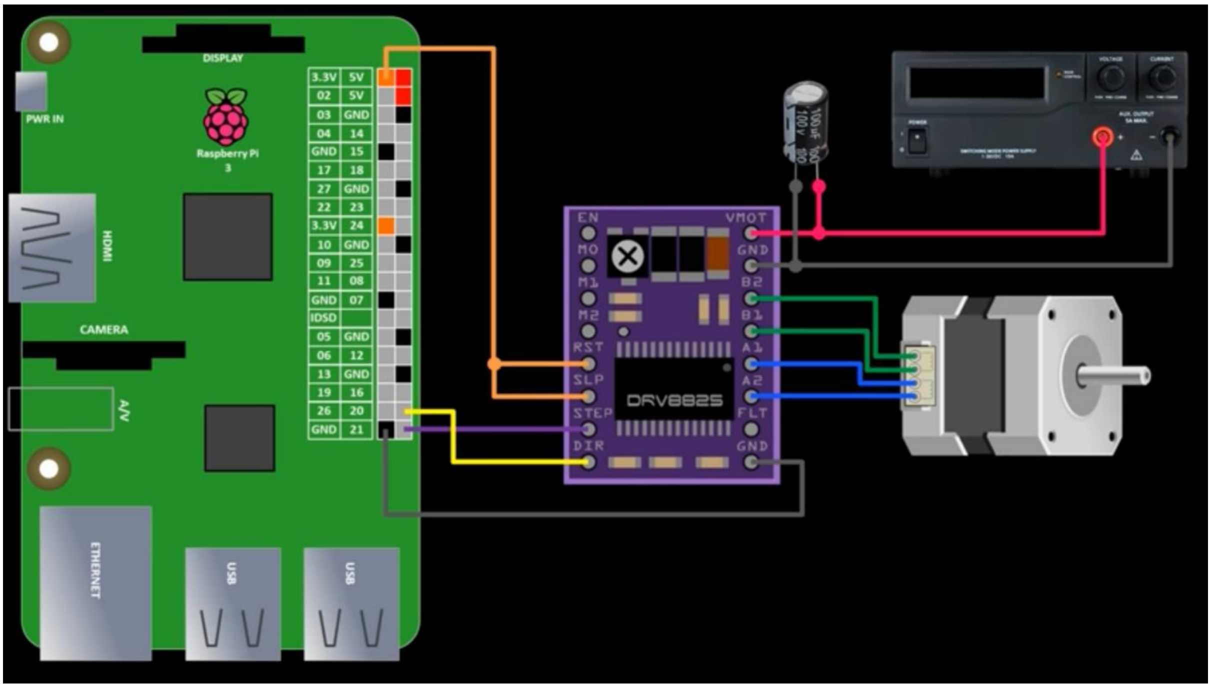

Figure 135 Ports and connections of motor driver

10 Computer vision

The approach to calculate the distance of the object from the camera is by using basic trigonometry and pixel distance. Before calculating the distance we need to know about the setup of the camera used. In this case we are using two web cameras in order to find the exact distance of the object from the camera setup. The two cameras are placed at a known distance to each other as shown in the Figure-136. D is the known distance between the two webcams.

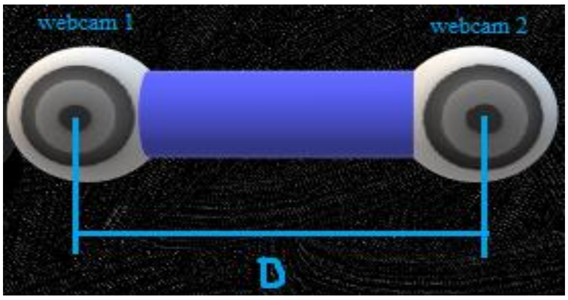

Figure 136 Stereo Camera Setup

To calculate the distance between the object and the camera setup, trigonometry can be used as an approach as shown in Figure-137.

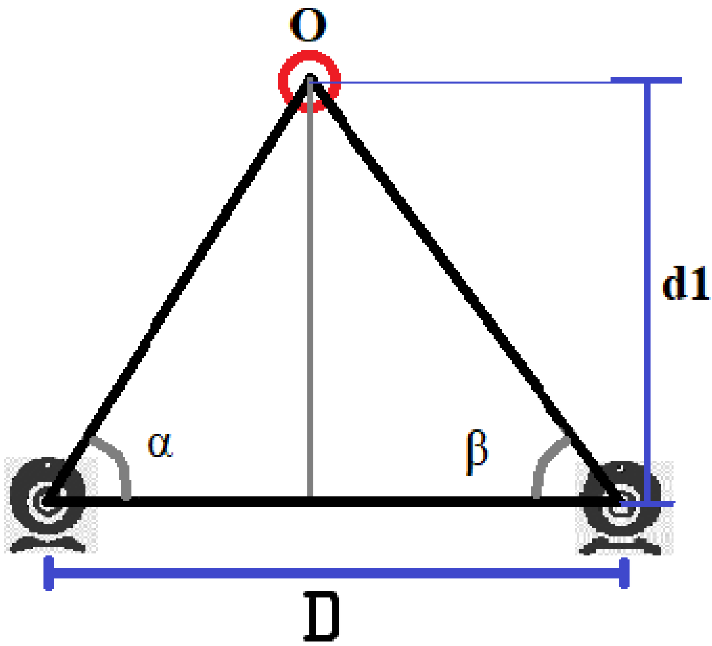

Figure 137 Distance calculation

In the above image the red circle marked as ‘O’ shows the position of the object detected by the camera. “d1” shows the distance to be calculated, “α” & “β” shows the angle projected by the line joining webcam 1 and webcam 2 with the object and ‘D’ shows the predefined distance between the two web cameras.

Using trigonometry the variable ‘d1’ can be calculated by rearranging the below Equation 11.

$$D = (\frac{d1}{\tan\alpha} + \frac{d1}{\tan\beta})$$

Equation 11 Distance

But to find ‘d1’, it is crucial to find the subtended angles “α” & “β”. They are found using the method as illustrated below:

The Figure-138 shows a field of vision marked by black lines and a frame of the camera marked using a rectangle projected at any random distance ‘d’. The red dot represents the position of the object detected. This is only for one axis and is repeated for all remaining axes by considering the changes in the specification of the camera due to orientation. Figure-138 shows the x axis calculations and the web camera with an angle of vision of 78 degrees and a pixel count of 640 in the x axis. The OpenCV packages from python are programmed as such to read the pixel number at which the object is positioned hence using this information the distance of the object from the center of the frame can be calculated as shown below:

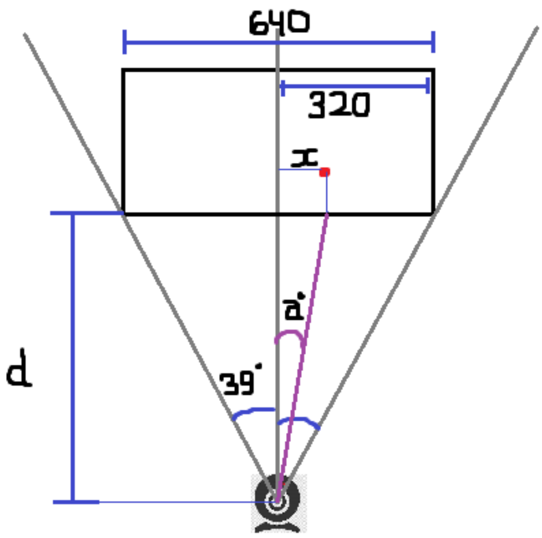

Figure 138 Angle Calculation in one Camera

$$320\ pixels \rightarrow 39°$$

$$1\ pixel \rightarrow \left(\frac{39}{320}\right)°$$

$$Angle\ 'a' = x\ pixels = (0.121875\ X\ x)°$$

Therefore by getting the numeric value of the number of pixels between the center of the field of vision and the object position from the camera, the angle ‘a’ (angle between the normal of the field of vision and the object position) can be determined **[10]**.

Using the method shown in the Figure- we can calculate the angles ‘α’ & ‘β’ and use them in the Equation-11. Rearranging the equation we get

$$d1 = D(\frac{1}{\tan \propto} + \frac{1}{\tan \beta})$$

Equation 12 Distance From Camera

11 Kinematics of the robot

11.1 Denavit Hartenberg Algorithm (DH Algorithm)

The Denavit Hartenberg algorithm will be used to find the transformation matrices and equations. The frame layout along with the required dimensions labelled are shown in Figure-139

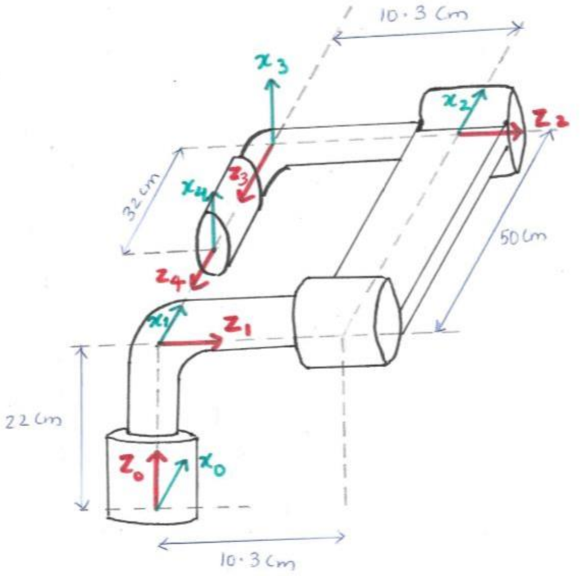

Figure 139 DH Robot Frame Layout

DH Table for the robot :

Table 15 DH table

Frame Number	θ	α	r	d
1	θ_1 (q)	90°	0	22
2	θ_2 (r)	0°	-50	10.3
3	θ_3(s)	-90°	0	-10.3
4	θ_4(t)	0°	0	32

Referring Table-13, the variables the robot offers for movement is θ_n(q,r,s,t). The Homogeneous Transformation matrix can be found using this table.

The general idea of the use of the homogeneous matrix is understood by the equation

$$^{0}T_4 \text{ x } ^{4}\text{P} = {}^{0}\text{P}$$

Equation 13 Transformation Equation

The 0^{th} frame is the base frame co-ordinate and the 4^{th} frame is the end effector frame as shown in Figure-139. Any point in the end effector frame can be found in respect to the base co-ordinate (0^{th} frame) which is fixed using which all the θ_n can be found.

T is the transformation or homogeneous matrix from 0^{th} frame to 4^{th} frame whose multiplication by the points **P** in frame **4** will produce the resulting co-ordinates of the same point in frame **0**.

${}^{0}T_4$ can be found using the values in Table-13. The values are filled in the matrix:

$$^{n-1}T_n = \begin{bmatrix} \cos\theta_n & -\sin\theta_n \cos\alpha_n & \sin\theta_n \sin\alpha_n & r_n \cos\theta_n \\ \sin\theta_n & \cos\theta_n \cos\alpha_n & -\cos\theta_n \sin\alpha_n & r_n \sin\theta_n \\ 0 & \sin\alpha_n & \cos\alpha_n & d_n \\ 0 & 0 & 0 & 1 \end{bmatrix}$$

'n' in the above matrix represents the figure is the frame number for which the DH matrix is written. Using this matrix we can calculate ${}^{0}T_1 {}^{1}T_2 {}^{2}T_3 {}^{3}T_4$ to give ${}^{0}T_4$

$$^{0}T_1 = \begin{bmatrix} \cos(q) & 0 & \sin(q) & 0 \\ \sin(q) & 0 & -\cos(q) & 0 \\ 0 & 1 & 0 & 22 \\ 0 & 0 & 0 & 1 \end{bmatrix} \qquad ^{1}T_2 = \begin{bmatrix} \cos(r) & -\sin(r) & 0 & -50\cos(r) \\ \sin(r) & \cos(r) & 0 & -50\sin(r) \\ 0 & 0 & 1 & 10.3 \\ 0 & 0 & 0 & 1 \end{bmatrix}$$

$$^{2}T_3 = \begin{bmatrix} -\sin(s) & 0 & -\cos(s) & 0 \\ \cos(s) & 0 & -\sin(s) & 0 \\ 0 & -1 & 0 & -10.3 \\ 0 & 0 & 0 & 1 \end{bmatrix} \qquad ^{3}T_4 = \begin{bmatrix} \cos(t) & -\sin(t) & 0 & 0 \\ \sin(t) & \cos(t) & 0 & 0 \\ 0 & 0 & 1 & 32 \\ 0 & 0 & 0 & 1 \end{bmatrix}$$

$$^{0}T_4 = {}^{0}T_1 {}^{1}T_2 {}^{2}T_3 {}^{3}T_4$$

Multiplying all the 4 matrices we get the transformation matrix from 0^{th} frame to 4^{th} frame.

$$^{0}T_4 = \begin{bmatrix} -\sin(q)\sin(t) - \sin(r+s)\cos(q)\cos(t) & -\sin(q)\cos(t) + \sin(t)\sin(r+s)\cos(q) & -\cos(q)\cos(r+s) & -50\cos(q)\cos(r) - 32\cos(q)\cos(r+s) \\ -\sin(q)\sin(r+s)\cos(t) + \sin(t)\cos(q) & \sin(q)\sin(t)\sin(r+s) + \cos(q)\cos(t) & -\sin(q)\cos(r+s) & -50\sin(q)\cos(r) - 32\sin(q)\cos(r+s) \\ s\cos(t)\cos(r+s) & -s\sin(t)\cos(r+s) & -\sin(r+s) & -50\sin(r) - 32\sin(r+s) + 22 \\ 0 & 0 & 0 & 1 \end{bmatrix}$$

Using Equation-13, any point in the end effector frame (4^{th} frame) with any angular orientation of the joints, the same point can be found with respect to the 0^{th} frame and vice-versa.**[11]**

11.2 Angular Orientation

Using the concept of inverse kinematics and the derived transformation matrix, the angular orientation of each joint can be found. The point with respect to the 0th frame which is the point where the end effector has to each is known. The point on the 4th frame is also known. The position of the 4th frame itself is decided by the angular orientation of each joint. Using this information we can deduce equations with the unknown angular joint variables which is used to find the joint angles.

Let the point in the 0th frame where the end effector is supposed to reach by denoted as ***x***, ***y*** and ***z*** variables

$$^{0}P = \begin{bmatrix} x \\ y \\ z \\ 1 \end{bmatrix}$$

The point in the end effector frame is taken as (0, 0, 0).

$$^{4}P = \begin{bmatrix} 0 \\ 0 \\ 0 \\ 1 \end{bmatrix}$$

On solving Equation-13, we get

$$\boldsymbol{x = -50\,Cos\,(q)\,Cos(r) - 32\,Cos\,(q)\,Cos(r + s)}$$

Equation 14

$$\boldsymbol{y = -50\,Sin\,(q)\,Cos(r) - 32\,Sin\,(q)\,Cos(r + s)}$$

Equation 15

$$\boldsymbol{z = -50\,Sin\,(r) - 32\,Sin\,(r + s) + 22}$$

Equation 16

The angular variables *q*, *r* and *s* decide the position of the end effector. The angular variable *t* is absent from all the three equations. This implies that *t* does not have any impact on the position of the end effector but the angular orientation of the end effector.

11.3 Camera Frame and Position

OpenCV package from python and the stereo camera depth detection method is used to map the co-ordinates of the object to be detected. To make the robot orient according to the position found, the co-ordinates of the point with respect to the camera must be found in the 0th frame of the robot through which all angles are found as mentioned in Heading 11.1.

Important Notes:

1) It is absolutely necessary that the distance between the placement of the camera and the robot must be same.
2) It is absolutely necessary that the orientation between the frames of the camera and the robot's 0^{th} frame must never change once calculations are done.

The main equation to focus on is:

$$^{0}T_{c} \times {}^{4}P = {}^{0}P$$

Equation 17

The $^{0}T_{c}$ transform matrix is the transformation matrix from frame 0^{th} to the position of the camera's frame '*c*'.

To find this matrix, counter clockwise rotation matrices and translation matrices will be used. The position of both the frame and the camera with respect to each other is shown in Figure-140

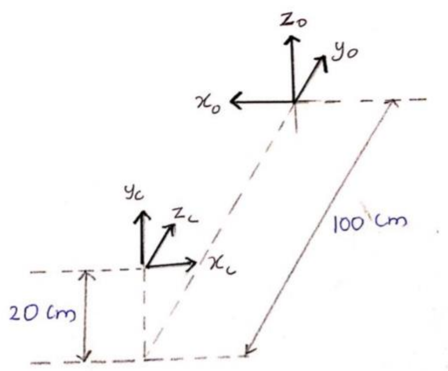

Figure 140 Robot and Camera Frame

They are kept at a distance of 100 cm apart for reasonable field of vision. The 0^{th} frame is on the ground level. The camera setup is 20 cm above the ground.

The order in which the transformation matrix will be calculated is:

1) Rotate frame 0 at -90º counter clockwise along the x direction with the translation part of the transform matrix kept 0.
2) Rotate the new position of the 0^{th} frame by 180º counter clockwise along the y axis with the translation of the transform matrix kept 0. .
3) Distance of the centres of both the frame (the latest position of the 0^{th} frame and the camera's frame is same) is filled into the last transform without any rotation components which is an identity matrix. The values for the translation are (0 , 20, -100) after reorienting the 0^{th} frame in the same direction as the camera's frame.

Multiplication of the 3 matrices in order will give the transformation matrix $^{0}T_{c}$. Counter clockwise rotation matrices along all the axis are given as:

$$R_x(\phi) = \begin{pmatrix} 1 & 0 & 0 \\ 0 & \cos\phi & \sin\phi \\ 0 & -\sin\phi & \cos\phi \end{pmatrix}$$

$$R_y(\theta) = \begin{pmatrix} \cos\theta & 0 & -\sin\theta \\ 0 & 1 & 0 \\ \sin\theta & 0 & \cos\theta \end{pmatrix}$$

$$R_z(\psi) = \begin{pmatrix} \cos\psi & \sin\psi & 0 \\ -\sin\psi & \cos\psi & 0 \\ 0 & 0 & 1 \end{pmatrix}$$

The translation matrix in a transform matrix without any rotation is given as:

$$\begin{bmatrix} 1 & 0 & 0 & t \\ 0 & 1 & 0 & u \\ 0 & 0 & 1 & v \\ 0 & 0 & 0 & 1 \end{bmatrix}$$

The values ***t, u*** and ***v*** are the translation values in *x*, *y* and *z* directions respectively.

The overall transform matrix can now be found by filling in the appropriate values as mentioned in points ***1, 2*** and ***3*** in the appropriate matrices and multiplying them in the order 1->2->3, we get:

$${}^{0}T_{c} = \begin{bmatrix} 1 & 0 & 0 & 0 \\ 0 & 0 & -1 & 0 \\ 0 & 1 & 0 & 0 \\ 0 & 0 & 0 & 1 \end{bmatrix} \begin{bmatrix} -1 & 0 & 0 & 0 \\ 0 & 1 & 0 & 0 \\ 0 & 0 & -1 & 0 \\ 0 & 0 & 0 & 1 \end{bmatrix} \begin{bmatrix} 1 & 0 & 0 & 0 \\ 0 & 1 & 0 & 20 \\ 0 & 0 & 1 & -100 \\ 0 & 0 & 0 & 1 \end{bmatrix}$$

$${}^{0}T_{c} = \begin{bmatrix} -1 & 0 & 0 & 0 \\ 0 & 0 & 1 & -100 \\ 0 & 1 & 0 & 20 \\ 0 & 0 & 0 & 1 \end{bmatrix}$$

On solving Equation-17 we can obtain the values of ***x, y*** and **z** in *Equation-14,15,16*.

Now that the values are found, the unknown angles ***q, r,*** and ***s*** can be found. The angular orientation of the last joint ***t*** is more or less fixed for the initial prototype.

12 Result and Conclusion

The task of building an industrial robot from scratch began with finding out the best and most efficient link arrangement, to defining joints, gearing arrangement, motion analysis to check if the design will provide the expected movement and stress analysing the design further for topological optimization to reduce the weight of the design as much as possible. The dimensions of the design were finalized based on the standard bearing dimensions available in the market. Bearing was absolutely necessary for smooth motion between the links. The computer design was then sent to a 3D printing vendor.

After the end of the design stage, various motors were studied that would provide actuation and then finalized. The required torque of the stepper motor at each joint was obtained during the motion analysis of the design. So the specifications of the stepper motor was estimated based on the analysis results.

Microcontrollers that will send data to the stepper motors and control their movement were analysed. Due to its drawbacks, stepper motor drivers were also required to direct the flow of power and make controlling of the stepper motors even easier. The drivers and controllers were selected as such that they were compatible with popular programming languages for ease of integration with computer vision programmes.

The next stage was to study object detection and tracking using cameras which is the input factor for the robot. Following this study was to integrate it with the kinematics of the robot. Method to find the joint variables to make the robot move accordingly was studied and implemented. The final stage was integrating the studied kinematics and the visual feedback from the cameras.

A basic 4 degree of freedom industrial robot is fabricated using 3D printing techniques and computer vision. It is artificially intelligent. Based only on visual feedback and without any human interaction, the robot can perform pick and place tasks.

13 Future Scope of research

Joint design can be further improved. The linkage of each of the adjacent links with one another can be made more concrete with easier assembly and sturdy linkage. Two more degree of freedom can be added to the design to make it more flexible and use it to the best of its capabilities and replicate human hand movement. Overall precision can be brought down by many times to perform delicate and intricate tasks. Apart from visual feedback, the option to make the robot perform tasks using sound and also integration of those sounds with computer vision is also possible. This technology can be further extended to medical robotics with extreme precision in guiding the doctors during critical operations or performing some tasks which are extremely delicate and as such a robot's accuracy is crucial which can have a major impact on the chances of survival than that of medical human hands.

14 References

[1] Md Hazrat Ali, Aizat K, Yerkhan K,Zhandos T.and Anuar O. 2018. Vision-based Robot Manipulator for Industrial Applications. In Proceedings of the International Conference on Robotics and SmartManufacturing (RoSMa2018), July 19 – 21, 2018, IIITDM Kancheepuram, Chennai, INDIA, https://www.sciencedirect.com/science/article/pii/S1877050918309694

[2] Mortexa Alebooyeh, R. Jill Urbanic. 2019. Neural Network Model for Identifying Workspace, Forward and Inverse Kinematics of the 7-DOF YuMi 14000 ABB Collaborative Robot. In proceeding of the IFAC (International Federation of Automatic Control) hosted by Elsevier ltd. Department of Mechanical, Automotive, and Materials Engineering, University of Windsor, Windsor, Ontario, Canada N9B

[3] RobotsWorx. A Scott Company. What Are The Main Types Of Robots?. Retrieved from https://www.robots.com/faq/what-are-the-main-types-of-robots

[4] Northwestern Robotics. 2017. Modern Robotics, Chapter 2.2: Degrees of Freedom of a Robot. Video. (26 August 2017) Retrieved October 25, 2019 from https://www.youtube.com/watch?v=zI64DyaRUvQ

[5] O.T. Vinta. 2018. Tutorial: How to Derive the Formula for the Planetary Mechanism Gear Ratio. Video. (09 January 2018). Retrieved November 12, 2019 from https://www.youtube.com/watch?v=9c1CyklAN5A

[6] Dr. Yang Cao. 2014. ENGR380 – Tutorial #6 (Feb. 17-21). Retrieved December 27, 2019 from https://drive.google.com/file/d/0B5meorzDrBfRUVAwQk1VeG1mVkk/view

[7] THOMAS. For Industry. Stepper Motors vs. DC Motors - What's the Difference?. Retrieved from https://www.thomasnet.com/articles/machinery-tools-supplies/stepper-motors-vs-dc-motors/

[8] How to Mechatronics. How a stepper motor works. Retrieved from https://howtomechatronics.com/how-it-works/electrical-engineering/stepper-motor/

[9] rdagger68. 2017. Raspberry Pi Stepper Motor Tutorial. Video. (04 June 2017). Retrieved February 18, 2020 from https://www.youtube.com/watch?v=LUbhPKBL_IU&t=611s

[10] Clayton Darwin. 2018. Distance (Angles+Triangulation) - OpenCV and Python3 Tutorial - Targeting Part 5. Video. (27 August 2018). Retrieved March 06, 2020 from https://www.youtube.com/watch?v=sW4CVI51jDY&t=689s

[11] Angela Sodemann. 2017. Robotics 1 U1 (Kinematics) S5 (HTM) P2 (HTM by Denavit Hartenberg). Video. (02 September 2017). Retrieved March 14, 2020 from https://www.youtube.com/watch?v=4WRhVqQaZTE&list=PLm0w6jo2iAInn2cfMbQNxAh5tfJszrLLX&index=5&t=0s

Robotic Arm Manipulator

ORIGINALITY REPORT

6%	1%	1%	6%
SIMILARITY INDEX	INTERNET SOURCES	PUBLICATIONS	STUDENT PAPERS

PRIMARY SOURCES

1	Submitted to Coventry University Student Paper	1%
2	livelig.com Internet Source	<1%
3	Submitted to University of Greenwich Student Paper	<1%
4	Submitted to University of Pretoria Student Paper	<1%
5	Submitted to University of Sheffield Student Paper	<1%
6	Submitted to American University of Beirut Student Paper	<1%
7	Submitted to University of Newcastle upon Tyne Student Paper	<1%
8	Submitted to University of Queensland Student Paper	<1%
9	Henry W. Stone. "Kinematic Modeling, Identification, and Control of Robotic	<1%

	Manipulators", Springer Nature, 1987 Publication	
10	Submitted to Central Queensland University Student Paper	<1%
11	Submitted to Institute of Technology, Sligo Student Paper	<1%
12	Submitted to The Hong Kong Polytechnic University Student Paper	<1%
13	Submitted to Swinburne University of Technology Student Paper	<1%
14	archive.org Internet Source	<1%
15	Morteza Alebooyeh, R. Jill Urbanic. "Neural Network Model for Identifying Workspace, Forward and Inverse Kinematics of the 7-DOF YuMi 14000 ABB Collaborative Robot", IFAC-PapersOnLine, 2019 Publication	<1%
16	Submitted to Wiltshire College Student Paper	<1%
17	Submitted to University of Newcastle Student Paper	<1%
18	edoc.pub Internet Source	

<1%

19	Submitted to Heriot-Watt University Student Paper	<1%
20	Submitted to Universiti Malaysia Perlis Student Paper	<1%
21	www.houstondad.com Internet Source	<1%
22	gtventic-shared.blogspot.com Internet Source	<1%
23	Submitted to University of Aberdeen Student Paper	<1%
24	GÖRan Selvik. "Roentgen stereophotogrammetry", Acta Orthopaedica Scandinavica, 2009 Publication	<1%
25	Submitted to Loughborough University Student Paper	<1%
26	Submitted to University of Utah Student Paper	<1%
27	Submitted to National University of Singapore Student Paper	<1%
28	Submitted to Rochester Institute of Technology Student Paper	<1%

29	Sandipan Bandyopadhyay, Ashitava Ghosal, Bahram Ravani. "A DIFFERENTIAL GEOMETRIC METHOD FOR KINEMATIC ANALYSIS OF TWO- AND THREE-DEGREE-OF-FREEDOM RIGID BODY MOTIONS*", Mechanics of Structures and Machines, 2002 Publication	<1%
30	Submitted to Runshaw College, Lancashire Student Paper	<1%
31	Submitted to Galway-Mayo Institute of Technology Student Paper	<1%
32	Submitted to University of Dehli Student Paper	<1%
33	Submitted to Chindwin College Student Paper	<1%
34	Submitted to Mar Baselios College of Engineering and Technology Student Paper	<1%
35	Submitted to AUT University Student Paper	<1%
36	Submitted to Bolton Institute of Higher Education Student Paper	<1%
37	Submitted to Grimsby College, South	<1%

Humberside
Student Paper

38	Submitted to Middle East Technical University Student Paper	<1%
39	Submitted to University of Kent at Canterbury Student Paper	<1%
40	Submitted to Institute of Technology, Nirma University Student Paper	<1%
41	Submitted to University of Hertfordshire Student Paper	<1%
42	Submitted to University of Wolverhampton Student Paper	<1%
43	Submitted to University of Sunderland Student Paper	<1%
44	Submitted to University of Lincoln Student Paper	<1%
45	Submitted to Cranfield University Student Paper	<1%
46	"Industrial and Robotic Systems", Springer Science and Business Media LLC, 2020 Publication	<1%
47	Submitted to University of Southampton Student Paper	<1%

48	www2.deloitte.com Internet Source	<1 %
49	Submitted to Papua New Guinea University of Technology Student Paper	<1 %
50	Submitted to Florida International University Student Paper	<1 %

Exclude quotes	On	Exclude matches	< 10 words
Exclude bibliography	On		

AMITY SCHOOL OF ENGINEERING & TECHNOLOGY

DEPARTMENT OF INFORMATION TECHNOLOGY

Parent's Feedback Form

Date: 18/05/2020

Name of the Student: ABHINAV SHARMA

Programme & Batch: B.TECH MECHANICAL ENGINEERING (2016-2020)

Enrollment No.: A2399816016

Name of the Father/Mother: CHANDER PARKASH

Organization: Moon Flight Support Pvt. Ltd.

Designation: MANAGING DIRECTOR

Contact Number: 9810393137 **E-mail ID: chandersharma72@gmail.com**

Please provide your comments on the following:

1. College Infrastructure : ☐ Excellent ■ Good ☐ Average ☐ Fair
2. Programme Curriculum : ☐ Excellent ☐ Good ■ Average ☐ Fair
3. Teaching Imparted to your ward : ☐ Excellent ■ Good ☐ Average ☐ Fair
4. Department resources : ☐ Excellent ■ Good ☐ Average ☐ Fair
5. Faculties Helpfulness : ☐ Excellent ■ Good ☐ Average ☐ Fair
6. Library Facilities : ☐ Excellent ■ Good ☐ Average ☐ Fair
7. Computing and Internet Facilities : ☐ Excellent ■ Good ☐ Average ☐ Fair
8. Personality/Communications Skills & Development Facilities : ☐ Excellent ■ Good ☐ Average ☐ Fair
9. Sports, Extra Curricular Facilities : ☐ Excellent ☐ Good ■ Average ☐ Fair
10. Placement Opportunities : ☐ Excellent ■ Good ☐ Average ☐ Fair
11. Transport Facilities : ☐ Excellent ■ Good ☐ Average ☐ Fair
12. Canteen Facilities : ☐ Excellent ■ Good ☐ Average ☐ Fair
13. Feedback on ward's Progress : ☐ Excellent ■ Good ☐ Average ☐ Fair
14. Discipline standards in the department : ☐ Excellent ■ Good ☐ Average ☐ Fair
15. Overall rating of the department : ☐ Excellent ■ Good ☐ Average ☐ Fair

Your feedback: Good facilities and infrastructure. A lot of opportunities for those who wish for success.

Your Suggestions for the improvement of Department: Curriculum of the initial years in Engineering dept.

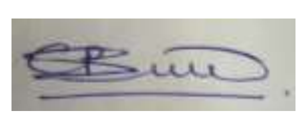

Signature

AMITY SCHOOL OF ENGINEERING & TECHNOLOGY

DEPARTMENT OF INFORMATION TECHNOLOGY

Parent's Feedback Form

Date: 18/05/2020

Name of the Student: RISHABH BAVITHRAN SC

Programme & Batch: B.TECH MECHANICAL ENGINEERING (2016-2020)

Enrollment No.: A2399816013

Name of the Father/Mother: R. SIVARAJAN

Organization: ADB

Designation: PROCUREMENT SPECIALIST

Contact Number: 9500416260 **E-mail ID: rsivarajan@hotmail.com**

Please provide your comments on the following:

1.	College Infrastructure	:	☐ Excellent	■ Good	☐ Average	☐ Fair
2.	Programme Curriculum	:	☐ Excellent	☐ Good	■ Average	☐ Fair
3.	Teaching Imparted to your ward	:	☐ Excellent	■ Good	☐ Average	☐ Fair
4.	Department resources	:	☐ Excellent	■ Good	☐ Average	☐ Fair
5.	Faculties Helpfulness	:	☐ Excellent	■ Good	☐ Average	☐ Fair
6.	Library Facilities	:	☐ Excellent	■ Good	☐ Average	☐ Fair
7.	Computing and Internet Facilities	:	☐ Excellent	■ Good	☐ Average	☐ Fair
8.	Personality/Communications Skills & Development Facilities	:	☐ Excellent	■ Good	☐ Average	☐ Fair
9.	Sports, Extra Curricular Facilities	:	☐ Excellent	☐ Good	■ Average	☐ Fair
10.	Placement Opportunities	:	☐ Excellent	■ Good	☐ Average	☐ Fair
11.	Transport Facilities	:	☐ Excellent	■ Good	☐ Average	☐ Fair
12.	Canteen Facilities	:	☐ Excellent	■ Good	☐ Average	☐ Fair
13.	Feedback on ward's Progress	:	☐ Excellent	■ Good	☐ Average	☐ Fair
14.	Discipline standards in the department	:	☐ Excellent	■ Good	☐ Average	☐ Fair
15.	Overall rating of the department	:	☐ Excellent	■ Good	☐ Average	☐ Fair

Your feedback: Good facilities and infrastructure. A lot of opportunities for those who wish for success.

Your Suggestions for the improvement of Department: Curriculum of the initial years in Engineering dept.

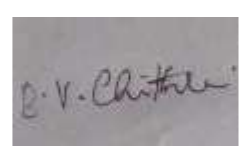

Signature

COMMENT BY EXTERNAL EXAMINER (Page to be added at the end of the Report)

Name of the External Examiner:
Signature: